Volume 14
Number 5
May 1975

# Inorganic Chemistry



Contribution from the School of Chemical Sciences,
University of Illinois, Urbana, Illinois 61801

## Electronic Structure of Various Ferricenium Systems as Inferred from Raman, Infrared, Low-Temperature Electronic Absorption, and Electron Paramagnetic Resonance Measurements

D. MICHAEL DUGGAN[1] and DAVID N. HENDRICKSON[2*]

*Received August 15, 1974* AIC40581F

Hexafluorophosphate and trichloroacetate ($TCA^-$) salts of decamethylferricenium ($DecaMFc^+$), 1,1'-dimethylferricenium ($DMFc^+$), and 1,1'-trimethyleneferricenium ($TMFc^+$) ions are studied with Raman, infrared, electronic absorption (20°K), and epr (12°K) spectroscopies. Raman and infrared data give the low-energy vibrational frequencies for the $^2E_{2g}$ ground states of the substituted ferricenium systems and these are compared with the corresponding frequencies for the $^1A_{1g}$ ground states of the substituted ferrocenes to ascertain qualitatively the relative importance of the $e_{2g}(d_{x^2-y^2}, d_{xy})$ orbital in ring–metal bonding. Resonance-enhanced symmetric ring–metal–ring stretches ($\nu_4$) are seen in the Raman spectra at 304 and 307 $cm^{-1}$, respectively, for the $PF_6^-$ and $TCA^-$ salts of unsubstituted ferricenium ion and it is concluded that the $e_{2g}$ orbital has little bonding involvement. Precession photography for $(DMFc^+)(TCA^-)\cdot TCAA$ shows that the $DMFc^+$ cation has its two rings situated such that the two methyl groups are positioned as far apart as possible; resonance Raman enhancement is only seen for $\nu_4$ at 322 $cm^{-1}$. In contrast, the methyl groups in $DMFc^+PF_6^-$ are eclipsed leading to resonance enhancement for $\nu_4$ at 327 $cm^{-1}$ and for the $C–CH_3$ deformation band at 311 $cm^{-1}$. TMFc has as strong features in the Raman spectrum a dominantly ring–metal–ring symmetric stretch at 329 $cm^{-1}$ and a "ring-torsion" mode at 246 $cm^{-1}$, while the corresponding bands for $(TMFc^+)(PF_6^-)$ are 316 and 218 $cm^{-1}$, respectively, and for $(TMFc^+)(TCA^-)\cdot 2TCAA$ are 311 and 216 $cm^{-1}$, respectively. Some $e_{2g}$ bonding is indicated for $TMFc^+$. Resonance Raman enhancement is seen for the $\nu_4$ and symmetric ring tilt bands in the $DecaMFc^+$ spectra: $PF_6^-$, 173 and 369 $cm^{-1}$, respectively; $TCA^-$, 167 and 365 $cm^{-1}$, respectively. The resonance Raman effect, as a function of laser exciting line, is discussed for various bands. The complex low-temperature vibrational structure seen for the $^2E_{1u}[e_{1u}^3a_{1g}^2e_{2g}^4] \leftarrow {}^2E_{2g}[e_{1u}^4a_{1g}^2e_{2g}^3]$ electronic transition is identified for the various substituted ferricenium ions and is used, *via* a comparison with frequencies for the $^1A_{1g}$ ferrocenes, in a discussion of the relative ring–metal bonding characteristics of the $e_{1u}$ (potentially metal $4p_x$ and $4p_y$) orbital. For many of the salts, transitions from the lowest energy $^2E_{2g}$ Kramers doublet to the two doublets of the $^2E_{1u}$ excited state are assigned and it is found that for all of the $TCA^-$ salts the $^2E_{1u}$ excited-state splitting ($\delta'$) due to low-symmetry distortion is 170–180 $cm^{-1}$, whereas for the $PF_6^-$ compounds the splitting is in excess of 200 $cm^{-1}$ in each case. As was previously[15] suggested for unsubstituted ferricenium systems, multiple (*e.g.*, generally four) electronic origins are clearly identifiable for most of the substituted ferricenium compounds. Possible explanations for the multiple origins are advanced in terms of inequivalent crystal sites or exciton interactions or low-energy librational modes. Epr results (X band, powders at ~12°K) are presented for the six substituted ferricenium compounds and the low-symmetry distortions ($\delta$) in the $^2E_{2g}$ ground states are evaluated. Because of a parallel between $\delta$ and $\delta'$ and the temperature independence of $\delta'$ as inferred from the electronic spectra, it is concluded, contrary to MCD and susceptibility work, that $\delta$ is not temperature dependent.

### Introduction

It has been said that ferrocene is the benzene of inorganic chemistry, which is a reasonable statement in light of the range and depth of physical and theoretical studies carried out on ferrocene and its simplest derivative the ferricenium ion.[3] The statement can also be said to reflect the fact that ferrocene is a fundamental structural unit and model compound for thousands of other organometallic systems. The physical and theoretical studies of ferrocene and ferricenium ion generally have as their objective the elucidation of the electronic structure of these two species. The relative energies of the ground and excited states can be determined, and these, in combination with such observables as vibrational frequencies for both ground and excited states, can be used to deduce the composition of the one-electron molecular orbitals. It is with this in mind that we have initiated (and herewith report the initial findings of) a study of a *selected* series of ferricenium ions resulting from oxidation of the ferrocenes

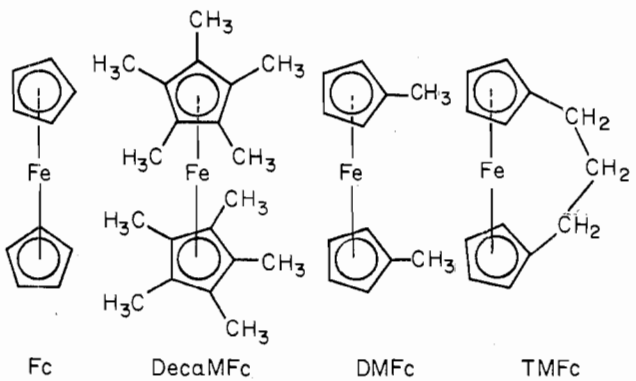


The three ferricenium ion derivatives incorporate ring substitutions that provide differing degrees of electronic and

geometric perturbations. For example, in comparison to the ferricenium ion, the decamethylferricenium ion (DecaMFc$^+$) is probably not geometrically distorted with respect to axial symmetry but the ring permethylation modulates the electronic properties of the rings (*i.e.*, inductive effects). The dimethylferricenium ion (DMFc$^+$) is asymmetrically substituted and this can lead to both geometric (ring tilting) distortions as well as electronic effects. The geometric distortion is seemingly increased in the 1,1'-trimethyleneferricenium ion (TMFc$^+$). We have elected to study these four ferricenium ions with Raman, infrared, low-temperature (~20°K) electronic absorption, and epr spectroscopies.

As indicated by magnetic susceptibility[4] and epr,[5-7] the electronic ground state of the ferricenium ion is a doublet, $^2E_{2g}[a_{1g}^2e_{2g}^3]$, where the one-electron molecular orbitals are probably dominantly d orbital in character: $a_{1g}(d_{z^2})$ and $e_{2g}(d_{x^2-y^2}, d_{xy})$ (the ferricenium ion is assumed to have $D_{5d}$ symmetry with the $z$ axis along the fivefold rotational axis). The details of fitting the magnetic properties of the ferricenium ion show that the $^2E_{2g}$ state is split into two Kramers doublets, $\psi\pm^a$ and $\psi\pm^b$, by spin–orbit interaction and low-symmetry distortions. Electron paramagnetic resonance[5-7] has been used to assess the low-symmetry distortion in the ground state. There is one low-lying excited state, the $^2A_{1g}[a_{1g}^1e_{2g}^4]$ state, with the "hole" in the $d_{z^2}$ level. The exact location of this state has not been determined;[4,8] in fact, the ordering of the $a_{1g}$ and $e_{2g}$ one-electron levels for ferrocene is still a matter of some dispute.[6,9-12] Of particular interest to this work is the $^2E_{1u}[e_{1u}^3a_{1g}^2e_{2g}^4]$ charge-transfer excited state where an electron is excited from the $e_{1u}$ orbital of the cyclopentadiene system to the $e_{2g}$ "hole" on the iron atom. This gives rise to the strong absorption band in the visible region which exhibits vibrational structure at low temperatures.[9,13-15] An analysis of the vibrational structure associated with the $^2E_{1u}$ excited state compared to that for both the ferricenium $^2E_{2g}$ ground state and the ferrocene $^1A_{1g}$ ground state can potentially lead to an understanding of the composition of the various molecular orbitals.[15] The $^2E_{1u}$ ferricenium state would also be expected to be split into two Kramers doublets, $\psi\pm^c$ and $\psi\pm^d$, by low-symmetry crystal fields. Recent low-temperature electronic absorption[9,13] and MCD studies[16,17] have detected such a splitting in the ferricenium $^2E_{1u}$ excited state.

With respect to the electronic structure of the ferricenium ion there are still many unanswered questions, some of which follow. (1) What is the energy separation between the $^2E_{2g}$ and $^2A_{1g}$ states, or, more properly, what are the energy separations between the $^2A_{1g}$ state and the two Kramers doublets from the $^2E_{2g}$ state? (2) What are the vibrational characteristics of the ferricenium $\psi\pm^a(^2E_{2g})$ and $^2E_{1u}$ (actually $\psi\pm^c$ and $\psi\pm^d$) states and how do they compare with each other and with that for the ground state of ferrocene? (3) As has been proposed in the susceptibility and MCD work, are the low-symmetry distortion parameters for the ferricenium $^2E_{2g}$ and $^2E_{1u}$ states temperature dependent? (4) Can Raman spectroscopy, *via* the resonance Raman effect (RRE), give any leads as to which vibrational modes are coupled to the $^2E_{1u} \leftarrow {}^2E_{2g}$ charge-transfer transition? Results bearing on questions 2–4 will be presented in this paper for the above series of four ferricenium ions.

## Experimental Section

**Compound Preparation.** Ferrocene, 1,1'-dimethylferrocene, and decamethylferrocene were obtained from commercial sources, while a sample of 1,1'-trimethyleneferrocene was obtained from Professor K. L. Rinehart.

All hexafluorophosphate salts were prepared by dissolution of the neutral molecules in concentrated sulfuric acid, followed by dilution with water (cooling in ice–water bath), filtration, and then addition to the filtrate of an aqueous solution of $NH_4PF_6$. The $PF_6^-$ salt immediately precipitates out in all cases and the analytical data in Table I[18] show that all $PF_6^-$ salts were obtained in reasonably pure form.

The trichloroacetate salts (TCA$^-$ = trichloroacetate and TCAA = trichloroacetic acid) were prepared in several ways, but the most general way is to dissolve the neutral molecule (~200 mg) in benzene and then to add ~600 mg of trichloroacetic acid dissolved in benzene resulting in a solution with a total volume of ~50 ml. Oxygen gas is bubbled through the solution for 15–20 min and then the flask is stoppered and set aside for 1–2 days. It will often be found that excellent crystals of the appropriate salt of the oxidized compound have grown on the walls of the container. A second batch of crystals may be obtained by decanting the mother liquor into a beaker where evaporation is allowed to proceed slowly over a period of 1 or 2 days. All trichloroacetate salts analyzed well with the exception of (DecaMFc$^+$)(TCA$^-$)·2TCAA, which is also the only compound that does not form exactly as described above. Instead of slowly crystallizing out of solution, the (DecaMFc$^+$)(TCA$^-$)·2TCAA product precipitates as a fine crystalline powder soon after addition of the acid. It was thought that the impurities in the sample of (DecaMFc$^+$)(TCA$^-$)·2TCAA might be some (DecaMFc$^+$)(TCA$^-$)·TCAA. Preparation of a DecaMFc$^+$ salt by dissolution of DecaMFc in concentrated $H_2SO_4$ followed by addition of a water solution of trichloroacetic acid gave a product which had an analysis consistent with (DecaMFc$^+$)(TCA$^-$)·TCAA. Although not reported in this paper, the low-temperature electronic spectrum of this compound indicated vibrational progressions of ~370 cm$^{-1}$, which is consistent with our observations on the TCA$^-$·2TCAA compound (*vide infra*). The strongest peak in the spectrum is at 8108 Å, which corresponds to a *valley* in the spectrum we report for the TCA$^-$·2TCAA compound, and it is concluded that this TCA$^-$·TCAA impurity is not present. It may be, however, that whatever amount of some impurity is present, it does give noticeable effects in the epr (*vide infra*). Additional ways of preparing trichloroacetate ferricenium salts are mentioned in our previous paper.[15]

**Physical Measurements.** Infrared spectra for all compounds were recorded on a Beckman IR-12 spectrometer. The samples were prepared as dilute 13-mm KBr pellets. The far-ir spectrum of a pellet of (DecaMFc$^+$)($PF_6^-$) was also studied to 200 cm$^{-1}$ with a Beckman IR-11 instrument.

Raman spectra were obtained using a Spex Model RS2 Ramalab system with a Coherent Radiation argon–krypton laser. Four laser lines could be used; they are in the blue (20,483 cm$^{-1}$), green (19,428 cm$^{-1}$), yellow (17,596 cm$^{-1}$), and red (15,443 cm$^{-1}$) regions of the visible spectrum. For most of the work in this paper the output power of the laser was quite low, on the order of 30–40 mW at the exit window (under optimum conditions it could reach 300–400 mW). The low power was generally due to deterioration of the dielectric mirrors, and resulted in a lowering of the quality of some of the spectra. Narrow band-pass interference filters were used to filter out all laser side bands which would interfere with the Raman spectrum. These filters cut the intensity of the laser line by roughly 75%. Because there was available no filter for the yellow line, the yellow line could only be used where the spectral peaks could be readily distinguished from the laser lines.

Raman samples were all prepared as pure (*no KBr*) 13-mm pressed pellets, which were mounted in a rotating sample holder which was purchased from Spex Inc. It was found that for the dark blue to green ferricenium compounds it was necessary to have the sample spinning in the laser beam in order to obtain any spectrum at all. Since many of the pressed samples had highly reflective surfaces, it was necessary to carefully adjust the positioning of the pellet such that only *scattered* light and *not reflected* light entered the slit.

The low-temperature electronic spectra were taken on a Cary Model 14 spectrophotometer. Two different methods were used to cool the samples: one employed a double-vacuum-jacketed glass dewar, and the other, a Cryogenics Technology, Inc., Spectrim Cryocooling Module. The former method allowed direct immersion of the sample into a reservoir of liquid helium (with a liquid nitrogen heat shield). Although bubbling of the coolants was a frequent problem with this method, sample temperatures as low as 4.2°K were available only with this setup. The Spectrim unit is a closed-cycle helium gas refrigerator which develops a cold-station temperature of ~16°K. The cold station is linked to the sample by a copper rod, and sample temperatures of 20°K are possible. All samples were prepared as KBr pellets (very thin with a small amount of compound in ~90 mg of KBr). Mounting of the 13-mm KBr pellets on the Spectrim unit

was accomplished by pressing them into a threaded holder which was made of chromium-plated copper. The metal surface in contact with the pellet was greased with thermal conducting grease. To ensure that the pelleting agent does not make a difference in the observed spectrum (*i.e.*, differences in molecular distortions), the spectrum of $(DMFc^+)(TCA^-)\cdot TCAA$ was also run as a CsI pellet. Results identical with those from the KBr pellet were obtained.

Electron paramagnetic resonance data were obtained using a Varian Model E-9 spectrometer with an Air Products Heli-tran liquid helium cooling device. The sample temperatures obtained with this unit were on the order of 12°K.

## Results and Discussion

Before describing the results a few words about the paper organization might be beneficial. After presenting data germane to the structural characteristics of the three substituted ferricenium ions, the low-energy vibrational frequencies, as deduced from infrared and Raman measurements, for the ground state, $\psi\pm^a(^2E_{2g})$, of the ferricenium systems will be presented. Electronic spectra for the various ferricenium systems will give a sounding as to some of the vibrational frequencies of the $^2E_{1u}$ charge-transfer excited state. In the esr section we will ascertain the low-symmetry distortion parameters for the $^2E_{2g}$ ground states and these parameters will be contrasted with the low-symmetry distortion parameters for the $^2E_{1u}$ excited states as deduced in the electronic spectroscopy. Throughout this adventure we will try to keep an eye to determining the orbital composition of the various one-electron molecular orbitals that are involved in our measurements.

**Geometry.** The structure of only one substituted ferricenium compound has been reported, that for 1,1'-dimethylferricenium triiodide.[19] The results are for the most part consistent with what would be expected from chemical intuition. As is found in the X-ray structural work[20,21] for unsubstituted ferricenium cations, the metal–ring distances are quite similar to those for ferrocene.[22] The average Fe–C distance in the 1,1'-dimethylferricenium ion is 2.07 Å which is insignificantly larger than the 2.05 Å found[23] in $(Fc^+)(TCA^-)\cdot 2TCAA$ or the 2.06 Å found[21] in $(Fc^+)(picrate^-)$. This constancy of Fe–C distance in going from ferrocene to ferricenium ion is, of course, a reflection of the fact that the $e_{2g}$ electrons are very weakly bonding. With respect to 1,1'-dimethylferricenium triiodide, it is curious that the methyl groups are eclipsed; the eclipsing leads to a 6.6° angle between the two ring planes. Whether this tilting is to be found in other salts of 1,1'-dimethylferricenium ion has not been discussed in the literature. It should be possible to observe other rotamers of this ion in salts with other anions.

Two different salts of the 1,1'-dimethylferricenium cation were prepared in this study: the $PF_6^-$ and a compound that analyzes as $(DMFc^+)(TCA^-)\cdot TCAA$ (see Table I[18]). The triiodide ion is too intensely colored to allow a thorough determination of the electronic absorption characteristics of any ferricenium counterion. A single crystal of $(DMFc^+)(TCA^-)\cdot TCAA$ was studied with X-ray precession photography. It was found that the space group is the orthorhombic *Cmca* (the centric choice) and by density measurement $\rho_{measd} = 1.62$ g/cm$^3$, which agrees with $\rho_{calcd} = 1.66$ g/cm$^3$ for four $(DMFc^+)(TCA^-)(TCAA)$ units in a unit cell of dimensions $a = 10.66$ Å, $b = 18.62$ Å, and $c = 10.82$ Å ($Z = 539.9$). Consideration of the symmetry properties of the *Cmca* space group[24] shows that, in order to put *only four* cationic molecules in a unit cell, they must be placed on either of two sets of special positions, ($^1/_2$, 0, 0) or (0, 0, 0,). The crystallographic point symmetry of each of these special positions is $2/m$, which requires that the molecule possess a twofold rotation axis and a perpendicular mirror plane. This requirement in turn says that the methyl groups *cannot* be eclipsed but must in fact be perfectly staggered, that is, 180° away from eclipsed as indicated in

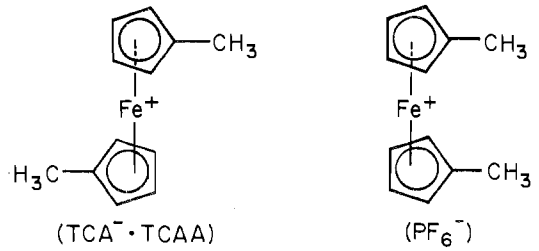


It is interesting that this would occur for it also requires the ring carbon atoms to be staggered and as such the rings will be more nearly parallel than in $(DMFc^+)(I_3^-)$. It should be pointed out that the $(DMFc^+)(TCA^-)\cdot TCAA$ system is unusual in that it crystallizes with only one TCAA. The structural work[23] on $(Fc^+)(TCA^-)\cdot 2TCAA$ and the analogous cobalticenium salt shows that in each compound two trichloroacetic acid molecules dimerize through the formation of hydrogen bonds and a third has been deprotonated to form the trichloroacetate anion. For $(DMFc^+)(TCA^-)\cdot TCAA$ it is an extraordinary bit of guesswork to suggest that a $TCA^-$ anion and a TCAA molecule have formed a dimer and that there is one dimer at each of the other four special positions.

For $(DMFc^+)(PF_6^-)$ there is *no* crystallographic evidence for any specific structure of the cation. Both $I_3^-$ and $PF_6^-$ are relatively rigid and it could be guessed that the cation in $(DMFc^+)(PF_6^-)$ has eclipsed rings in analogy with $(DMFc^+)(I_3^-)$. Some support for this proposal will be presented in later sections (*e.g.*, see the epr section).

Conclusions as to the structure of the 1,1'-trimethyleneferricenium cation are easier to reach. In contrast to the situation with the other cations, the ring substitution in $TMFc^+$ prevents rotation of one ring relative to the other. It would be desirable to know the angle between the ring planes in $TMFc^+$. Although no structural work has been reported for an unsubstituted 1,1'-trimethylene-bridged metallocene, the structure[25] of α-keto-1,1'-trimethyleneferrocene is of use. Since the rings in this substituted ferrocene are tilted at an angle of 8.8° and because models suggest that the deviation from ring parallelism should be greater for TMFc than for the α-keto compound, we suggest that the $TMFc^+$ cation has the greatest ring nonplanarity of the ferricenium systems considered in this work and that the rings are tilted by ~9°. It may be expected that there will not be a large difference in the $TMFc^+$ structures for the two salts prepared ($PF_6^-$ and $TCA^-\cdot 2TCAA$). Support for this statement will be given in the epr section.

It is very probable that the $DecaMFc^+$ cation in its compounds shows nearly perfect axial symmetry and no ring tilting.

As set out above, the observed geometric distortions for the three substituted ferricenium ions will give us some qualitative guide as to expected trends in low-symmetry distortion parameters; however, it *cannot* be expected that complete transferability will be found. There is a possibility of dynamic Jahn–Teller distortions in these ferricenium systems.

**Vibrational Spectra.** In this section the ground-state vibrational modes of each of the four ferricenium systems will be discussed. Of major concern will be those gerade low-energy modes which might appear as vibrational structure on the $^2E_{1u} \leftarrow {}^2E_{2g}$ charge-transfer electronic absorption band. It is generally quite informative to know the type of vibration coupled to an observed electronic transition.

No fewer than eight papers have been published emphasizing various aspects of the ir and Raman spectra of ferrocene,[26–33] while only a few[34–36] have discussed the ferricenium ion, and these have only been infrared studies. *A Raman spectrum of the ferricenium cation has not been reported.* The frequencies of the gerade vibrational modes of ferrocene and their descriptions are given in Table II. The $^2E_{1u}$ excited-state analogs

**Table II.** Reported Frequencies for the Gerade Vibrational Modes of Ferrocene[a]

| Symmetry | Designation | Ref 28 | Ref 30 | Ref 29 | Ref 33 | Ref 26 | Description |
|---|---|---|---|---|---|---|---|
| $A_{1g}$ | $\nu_1$ | 3100 | 3109 | 3112 | | 3110 | Sym CH str |
| | $\nu_2$ | 812 | 845 | 815 | | 814 | Sym CH ⊥ bend |
| | $\nu_3$ | 1105 | 1102 | 1106 | 1106 vs | 1102 | Sym ring breathing |
| | $\nu_4$ | 301 | 309 | 311 | 311 vs | 309 | Sym ring–metal str |
| $A_{2g}$ | $\nu_7$ | | 1096 | | | 1250 | CH ∥ def |
| $E_{1g}$ | $\nu_{12}$ | 3085 | 3100 | 3089 | | 3086 | CH str |
| | $\nu_{13}$ | 999 | 998 | 1001 | 997 w | 998 | CH ∥ bend |
| | $\nu_{14}$ | 835 | 815 | 815 | | 844 | CH ⊥ bend |
| | $\nu_{15}$ | 1412 | 1410 | 1414 | | 1410 | Sym C–C str |
| | $\nu_{16}$ | 390 | 389 | 393 | 395 vs | 389 | Sym tilt |
| $E_{2g}$ | $\nu_{23}$ | 3070 | 3088 | 3103 | | 3100 | CH str |
| | $\nu_{24}$ | 1175 | 1191 | 1197 | | 1191 | CH ∥ bend |
| | $\nu_{25}$ | 1059 | 1059 | 1062 | 1060 w | 1058 | CH ⊥ bend |
| | $\nu_{26}$ | 1356 | 1356 | 1358 | | 1356 | CC str |
| | $\nu_{27}$ | 892 | 897 | | | 897 | ∥ ring distortion |
| | $\nu_{28}$ | 600 | 597 | 600 | | 597 | ⊥ ring distortion |

[a] Frequencies are in $cm^{-1}$.

of the low-energy modes $\nu_4$ (symmetric ring–metal stretch), $\nu_{16}$ (symmetric ring tilt), and $\nu_{28}$ (⊥ ring distortion) are each likely candidates to appear as vibrational structure on the $^2E_{1u} \leftarrow {}^2E_{2g}$ transition and, as such, particular attention will be paid them. Comparisons will be made in this section between the ferrocene frequencies and whatever ferricenium ground-state frequencies that can be identified.

The infrared spectra reported[34-36] for the ferricenium ion have two rather curious features, one being that the number of strong bands is noticeably reduced from the number found for ferrocene. The other puzzle lies in the location of the asymmetric ring–metal–ring stretch. This band has been assigned as a *strong* band at 478 $cm^{-1}$ for ferrocene; however, for the ferricenium ion this band has been assigned[35,36] as a moderately intense band in the region of 405–423 $cm^{-1}$. Such a large shift in position in going from ferrocene to ferricenium seems inconsistent with the proposed nonbonding or weakly bonding character of the $e_{2g}$ molecular orbital. With respect to the overall charge on the ferricenium ion, it should be noted that the asymmetric ring–metal–ring stretch for $d^6$ cobalticenium *ion* has been located[29] at 455 $cm^{-1}$. As an alternative explanation for the appearance of the ferricenium ir spectrum we suggest that this asymmetric ring–metal–ring stretch band is greatly decreased in intensity in going from ferrocene to ferricenium ion. This suggestion is substantiated by the Raman spectra for $(Fc^+)(PF_6^-)$ and $(Fc^+)(TCA^-)\cdot 2TCAA$ which are reproduced in Figure 1 along with the Raman spectrum for $KPF_6$. The most intense feature found in both of the $Fc^+$ spectra is undoubtedly $\nu_4$, the symmetric ring–metal stretch, and because it is found at essentially the same position as found in ferrocene (see Table II), it is very reasonable to expect the asymmetric ring–metal–ring stretch for $Fc^+$ to be close to that found for ferrocene. It is known that the structure of the ferricenium ion is negligibly different from the structure of ferrocene, so it seems that some rearrangement of charge has taken place such that the dipole derivatives with respect to metal–ring modes have been decreased. In Table III[18] are given the low-energy Raman data obtained for the various ferricenium compounds as well as data for a cobalticenium salt and it can be seen that the Raman data ($\nu_4$ 315, $\nu_{16}$ 386, and $\nu_{28}$ 585 $cm^{-1}$) for the latter $d^6$ salt are similar to those for the $d^5$ salts.

It is interesting that in the Raman spectrum of the ferricenium ion very few bands are observed. This is not, however, related in cause to the ir phenomenon just discussed. On the contrary, it is supposed that the $\nu_4$ symmetric stretch is the strongest band due to resonance enhancement brought about by lasing the sample near the ring-to-metal charge-transfer electronic transition. Were it not for this effect, it is likely that, due to the deep color of these salts, no spectrum would be observable. We will discuss this apparent resonance Raman effect further in a latter section.

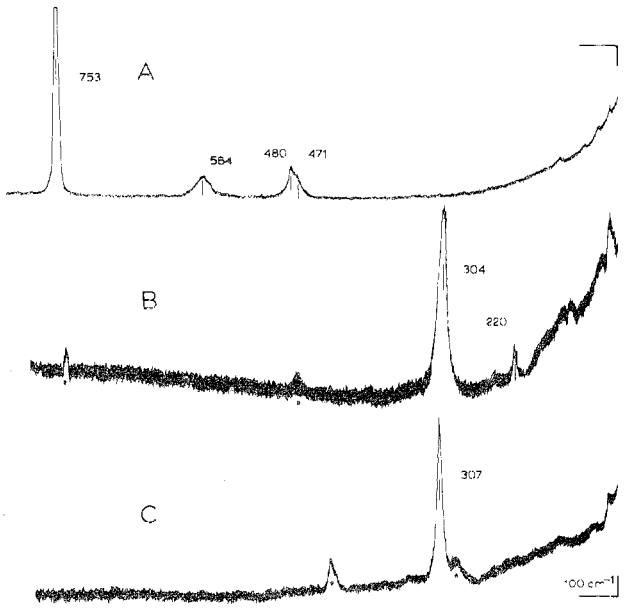


Figure 1. Raman spectra of rotating pressed pellets of $KPF_6$ (A), $(Fc^+)(PF_6^-)$ (B), and $(Fc^+)(TCA^-)\cdot 2TCAA$ (C). In the latter two spectra solid dots designate counterion peaks.

Understanding the ground-state vibrational structure of 1,1'-dimethylferrocene and its oxidized salts is made relatively straightforward by the study of Bailey and Lippincott[36] where the Raman and ir data for 1,1'-dimethylferrocene are presented and assigned. A comparison of their observed frequencies with the bands in the ir spectra of $(DMFc^+)(PF_6^-)$ and $(DMFc^+)(TCA^-)\cdot TCAA$ (see Figure 2[18]) shows that all the ring fundamentals are easily observable. However, the very strong $\nu_{11}$ asymmetric ring–metal–ring stretch in the neutral molecule at 482 $cm^{-1}$ now is at most a weak band in the $DMFc^+$ compounds, and the same may be said for the asymmetric tilting vibration seen at 496 $cm^{-1}$ in the neutral molecule. Again it must be assumed that some intensity-reducing mechanism is in effect in $DMFc^+$ for the metal–ring modes, especially as there are *no* strong bands in the low-frequency ir spectrum to 300 $cm^{-1}$ but also because, as is shown in Figure 3, in the Raman spectra for $(DMFc^+)(PF_6^-)$ and $(DMFc^+)(TCA^-)\cdot TCAA$ many of the low-energy bands for $DMFc^+$ appear where they were found[36] in the neutral molecule (only the lower energy regions of the Raman spectra are shown because only very weak bands are seen at higher energies).

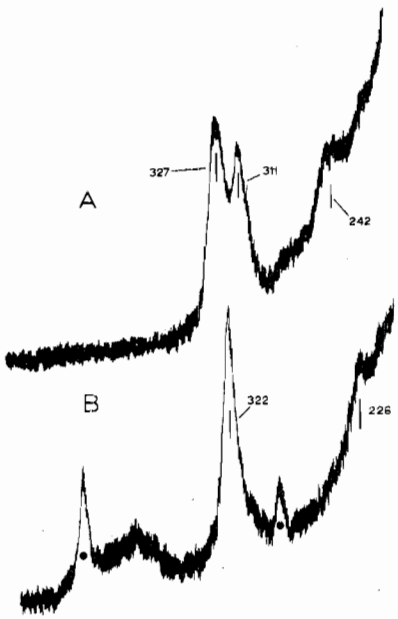


**Figure 3.** Raman spectra of rotating pressed pellets of $(DMFc^+)(PF_6^-)$ (A) and $(DMFc^+)(TCA^-)\cdot TCAA$ (B). The solid dots indicate counterion peaks.

The differences between the low-energy Raman spectra of $(DMFc^+)(PF_6^-)$ and $(DMFc^+)(TCA^-)\cdot TCAA$ are interesting and seem to be explicable in light of the differences in molecular structure of the cation in these two compounds. In the "trans" configuration that is indicated for the cation in $(DMFc^+)(TCA^-)\cdot TCAA$, the C–$CH_3$ deformation vibration, observed by Lippincott[36] at 330 $cm^{-1}$ as a strong band in the neutral molecule, would *not* be strongly coupled to the $^2E_{1u} \leftarrow {}^2E_{2g}$ ring-to-metal charge-transfer transition. If the C–$CH_3$ deformation mode has no energy contribution from metal–ring stretching, then there will be no mechanism of resonance enhancement of this band by exciting the Raman scattering at the frequency of the $^2E_{1u}$ transition and the C–$CH_3$ deformation band will be weak. The band at 322 $cm^{-1}$ in the Raman spectrum of $(DMFc^+)(TCA^-)\cdot TCAA$ can be assigned as $\nu_4$, the symmetric stretch.

The Raman spectrum of $(DMFc^+)(PF_6^-)$ is not only consistent with but offers support for the previous discussions. There is a symmetric stretch at 327 $cm^{-1}$ and the band at 311 $cm^{-1}$ is the C–$CH_3$ deformation mode, which, because there is inter-ring methyl–methyl repulsion, would be coupled to the symmetric ring–metal–ring stretch. The two motions are mixed, leading to resonance enhancement of both. The low-energy Raman bands observed at 242 $cm^{-1}$ ($PF_6^-$) and 226 $cm^{-1}$ ($TCA^-$) are most likely the 1,1'-dimethylferricenium counterparts of the weak 268-$cm^{-1}$ ring torsion mode observed for 1,1'-dimethylferrocene and assigned[36] as a ring torsion mode. It is anticipated that this torsion vibration may be more noticeable in the Raman spectrum of 1,1-trimethyleneferrocene.

The ir spectra of TMFc, $(TMFc^+)(PF_6^-)$, and $(TMFc^+)(TCA^-)\cdot 2TCAA$ are shown in Figure 4.[18] When they are not masked by counterion bands, most of the cyclopentadiene and trimethylene bridge bands that are observed in TMFc are also visible for $TMFc^+$. Again, as above, the low-energy ring–metal–ring bands either are missing or are of lowered intensity. Although the number of low-energy features makes any individual assignments uncertain, it is clear that $(TMFc^+)(PF_6^-)$ has no observable low-energy bands and only the cluster at ~500 $cm^{-1}$ is found for the $TCA^-$ compound and this is probably not a ring–metal–ring vibration. The low-energy Raman spectra for these same three compounds are reproduced in Figure 5 (only very weak bands are seen

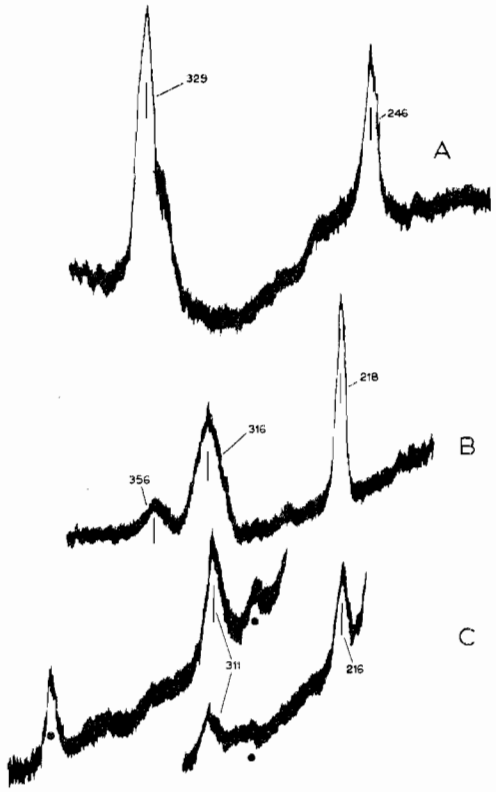


**Figure 5.** Raman spectra of rotating pressed pellets of TMFc (A), $(TMFc^+)(PF_6^-)$ (B), and $(TMFc^+)(TCA^-)\cdot 2TCAA$ (C). The solid dots designate counterion peaks.

at higher energies). Only two low-energy Raman bands are observed for TMFc, one at 329 $cm^{-1}$ which is very strong and shouldered at low energy and a medium-intensity band at 246 $cm^{-1}$. The higher energy band is assigned as a mode that is dominantly a symmetric ring–metal–ring stretch, but with a little bridge deformation mixed in. As proposed for the $DMFc^+$ systems, the lower energy band is possibly a modified ring torsion mode. Due to the tilt of the rings and the interconnection *via* the bridge any twisting of the rings will probably involve some deformation of the metal–ring vectors as well. Thus, for the $(TMFc^+)(PF_6^-)$ and $(TMFc^+)(TCA^-)\cdot 2TCAA$ compounds the torsion bands have increased intensities relative to the $\nu_4$ bands. The "torsion bands" also seem to be sharper than $\nu_4$ in the $TMFc^+$ salts.

The frequencies of the Raman bands for $(TMFc^+)(PF_6^-)$ and $(TMFc^+)(TCA^-)\cdot 2TCAA$ relative to those for TMFc are somewhat revealing. The $\nu_4$ stretch is decreased by 13 and 18 $cm^{-1}$ in the $PF_6^-$ and $TCA^-$ salts, respectively, as compared to TMFc. Perhaps this is evidence that the $e_{2g}(d_{xy}, d_{x^2-y^2})$ metal orbital is now more bonding with the ring than when the rings were planar. Furthermore, the torsion mode in the oxidized systems is at 28 $cm^{-1}$ lower energy in both cases than was found for TMFc, again implicating $e_{2g}$ participation in the bonding. A complete normal-coordinate analysis is needed to check that these shifts are not just due to "mixed" modes.

The ir spectrum of DecaMFc, heretofore unreported, is illustrated in Figure 6[18] along with ir spectra for $(DecaMFc^+)(PF_6^-)$ and $(DecaMF^+)(TCA^-)\cdot 2TCAA$. Infrared and Raman peaks found above 600 $cm^{-1}$ are given in Table IV; the more important region of the spectrum, for this work that below 600 $cm^{-1}$, is reported separately in Table V, where two possible assignments are given. Comparison of the ir spectra of DecaMFc and $DecaMFc^+$ shows that there are only small changes in the high-energy region. The relative intensities of the $\nu_{CH_3}$ *vs.* $\delta_{CH_3}$ and CC modes are interesting, but in no case is there a difference such as would imply a major change in structure. It is remarkable that all of the sub-

**Table IV.** Infrared and Raman Bands for DecaMFc and DecaMFc$^+$ Salts above 600 cm$^{-1}$

| DecaMFc | | (DecaMFc$^+$)(PF$_6^-$) | | (DecaMFc$^+$)(TCA$^-$)·2TCAA | |
|---|---|---|---|---|---|
| Raman | Ir | Raman | Ir | Raman | Ir |
| 3002 w | 2980 s | | 3000 mw | | 2990 mw |
| 2963 m | 2960 s | | 2975 mw | | 2982 mw |
| 2941 m | 2910 vs | 2925 m | 2910 m | 2925 m | 2920 m |
| 2887 vs | 2865 s | | | | 2860 sh |
| 2611 vs | 2715 w | | 2875 sh | | |
| 2176 vw | | | | | |
| 1476 m | 1478 m | | 1478 ms | | 1480 s |
| 1449 m | 1452 m | 1423 m | 1460 sh | 1423 m | 1460 sh |
| 1425 s | 1428 m | | 1428 mw | | 1430 mw |
| 1386 m | 1378 s | | 1395 s | | 1392 s |
| 1367 m | | | 1385 s | | 1386 s |
| 1225 w | | | | | |
| 1068 vw | 1075 mw | 1030 w | 1075 mw | 1030 w | 1080 mw |
| 1036 w | 1032 ms | | 1030 ms | | 1038 ms |
| 794 w | | | | | |

600-cm$^{-1}$ ir vibrations are still visible in going from DecaMFc to DecaMFc$^+$. The shift in position of any of the four bands is less than ~20 cm$^{-1}$ and this again adds further support to the proposal that the asymmetric ring–metal–ring stretch is *not* shifted by 70 cm$^{-1}$ in going from ferrocene to ferricenium ion.

Before assignments are given for the low-energy vibrational bands, it is useful to consider the Raman spectra of these three compounds as shown in Figure 7. For DecaMFc an excellent, well-resolved Raman spectrum can be obtained relatively easily. Apparently, the same four low-energy bands are seen as were seen in the infrared spectrum. The 515-cm$^{-1}$ ir band is tentatively associated with the 550-cm$^{-1}$ Raman band; similar shifts in band positions from the infrared to the Raman spectra are not observed for the other three peaks. The intensity and position of the 590-cm$^{-1}$ DecaMFc Raman band indicate it to be the perpendicular ring deformation mode, designated $\nu_{28}$ for ferrocene. In addition to this perpendicular ring deformation mode, there are four other modes expected in the low-energy region: the asymmetric and symmetric ring tilting modes and the asymmetric and symmetric ring–metal–ring stretching vibrations. In ferrocene the asymmetric modes are always at higher frequency than their symmetric counterparts and the ring tilts are higher in energy than the stretches. The DecaMFc bands at ~376 and ~453 cm$^{-1}$ show an alternation in intensity in passing from the ir to the Raman spectrum. For assignment no. 1 in Table V, we have taken the 453-cm$^{-1}$ band, which is the strongest ir band and a fairly weak Raman band, as the asymmetric stretch; the symmetric tilt is assigned to the 373-cm$^{-1}$ band which is more intense in the Raman than in the ir spectrum; and, the ~530-cm$^{-1}$ band is assigned to the asymmetric tilting mode which may well be at higher energy than found in ferrocene (492 cm$^{-1}$) due to the interaction of the methyl groups. If this assignment is correct, then the symmetric stretch $\nu_4$ is to be found at even lower frequencies and as such the ~180-cm$^{-1}$ band is tentatively assigned as $\nu_4$. To check this possibility an approximate

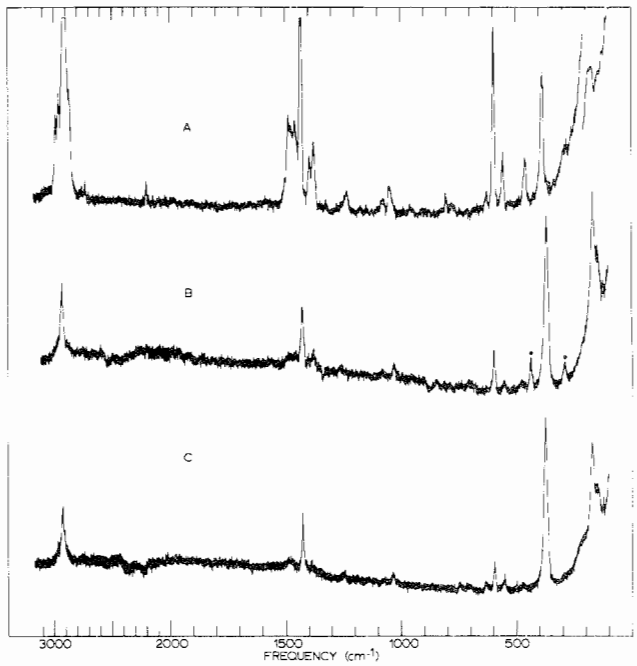


**Figure 7.** Raman spectra of rotating pressured pellets of DecaMFc (A), (DecaMFc$^+$)(TCA$^-$)·2TCAA (B), and (DecaMFc$^+$)(PF$_6^-$) (C). The counterion peaks are indicated by solid dots.

calculation of expected symmetric and asymmetric stretching frequencies for DecaMFc was carried out using the same metal–ring force constant $k$ and interaction constant $k_{12}$ as were found for ferrocene and changing only the mass of the rings. For an $XY_2$ molecule the analytical expressions for the symmetric and asymmetric vibrational frequencies are given by Herzberg[37] as

$$\nu_s = [(k + k_{12})/0.589M_Y]^{1/2}$$

$$\nu_a = [(1 + 2M_Y/M_X)((k - k_{12})/0.589M_Y)]^{1/2}$$

In these expressions $M_Y$ and $M_X$ are the masses of Y (the permethylated ring) and X (the iron atom). In the case of ferrocene, values of $k$ = 3.14 and $k_{12}$ = 0.56 mdyn/Å with masses appropriate for ferrocene give $\nu_a$ 473 and $\nu_s$ 311 cm$^{-1}$, which are close to the experimental values. Using the same force constants for DecaMFc leads to $\nu_a$ 436 and $\nu_s$ 220 cm$^{-1}$. It can be seen that small adjustments in $k$ and $k_{12}$ would give the assignment no. 1 experimental peaks of $\nu_a$ 453 and $\nu_s$ 180 cm$^{-1}$.

In the alternative assignment no. 2 for DecaMFc the strong and weak ir bands at 455 and 375 cm$^{-1}$ are taken to be the $\nu_a$ and $\nu_s$ vibrations. If the asymmetric tilt is assigned as above, then either the symmetric tilt is not observed in either the ir or the Raman spectrum or it is coincidentally degenerate with another band. Calculating the metal–ring force constants that would be required for assignment 2 gives $k$ = 7.11 and $k_{12}$ = 4.31 mdyn/Å. Force constants are determined not only by orbital overlap and bonding considerations but also by nuclear

**Table V.** Low-Energy Infrared and Raman Bands for DecaMFc and DecaMFc$^+$ Compounds

| DecaMFc | | (DecaMFc$^+$)(PF$_6^-$) | | (DecaMFc$^+$)(TCA$^-$)·2TCAA | | | |
|---|---|---|---|---|---|---|---|
| Raman | Ir | Raman | Ir | Raman | Ir | Assignment 1[b] | Assignment 2[b] |
| 169 w | | 173 ms[a] | | 167 ms[a] | | $\nu_s$ | |
| 179 w | | 218 w, br | | | | | |
| 285 w | | 283 w | | | | | |
| 378 ms | 375 m | 369 s[a] | 355 mw | 365 s[a] | 355 mw | Sym ring tilt | $\nu_s$ |
| 451 mw | 455 s | | 454 mw | (466) | 454 mw | $\nu_a$ | $\nu_a$ |
| 550 mw | 515 mw | 546 mw | 536 mw | ~546 | 536 mw | Asym ring tilt | Asym ring tilt |
| 590 s | 595 w | 599 w | 595 w | 593 mw | 595 w | ⊥ def | ⊥ def |
| 618 mw | | 625 | | | | | |

[a] Bands appear to be resonance enhanced in intensity. [b] $\nu_s$ and $\nu_a$ are the symmetric and asymmetric ring–metal–ring stretches.

and electron cloud repulsions; however, it is *not* anticipated that the inter-ring methyl interactions would lead to such a large interaction constant. Assignment 2 is probably incorrect; assignment 1 will be further substantiated as we now turn to the Raman spectra of DecaMFc$^+$ salts.

In reference to assignment 1, the Raman vibrations of (DecaMFc$^+$)($PF_6^-$) and (DecaMFc$^+$)($TCA^-$)·2TCAA (see Figure 7) show that in each spectrum *two* bands are resonance enhanced. The two enhanced bands are the symmetric tilting band at ~367 cm$^{-1}$ and the symmetric ring–metal–ring stretch at ~180 cm$^{-1}$. In all of the systems discussed in this paper this is the best example of resonance enhancement. The fact that these two bands have been assigned as symmetric modes is in keeping with the coupling of only symmetric modes to the $^2E_{1u} \leftarrow {}^2E_{2g}$ transition. Tilting of the rings in DecaMFc$^+$ would probably be coupled, as in the case of DMFc$^+$, to ring–metal–ring stretching; both mixed modes are somewhat resonance Raman enhanced.

A closer look can be taken at the supposed resonance Raman effect as it is occurring in these DecaMFc$^+$ compounds. The most unified body of work on the theory of the resonance Raman effect (RRE) over the past 1.5 decades has been presented by Albrecht and coworkers.[38-41] In the Raman spectrum of a molecule the intensity of a given line may be expressed as a function of the polarizability tensor, $\alpha_{\rho\sigma}$. The polarizability tensor can be written as a sum of three terms, $\alpha_{\rho\sigma} = A + B + C$. The $C$ term has been shown[38-41] to be in general quite small. The $B$ term is associated with Raman scattering through the presence of two vibronically coupled excited states, $|e^\circ\rangle$ and $|s^\circ\rangle$. Both of the electronic transitions from the ground state, $|g^\circ\rangle$, to these two excited electronic states need to be electric dipole allowed. Greatly enhanced Raman scattering occurs when the laser exciting frequency approaches the energy of the $g^\circ \rightarrow e^\circ$ or $g^\circ \rightarrow s^\circ$ electronic transitions. Those vibrational modes that most strongly couple to the electronic transition will be most highly resonance enhanced.

The $A$ term represents the case of Raman scattering off one excited electronic state, $|e^\circ\rangle$. In this case, it is also required that the $g^\circ \rightarrow e^\circ$ transition be electric dipole allowed. The difference in the $A$ and $B$ mechanisms is detectable experimentally due to the difference in frequency factors. The two frequency factors may be written

$$F_A = \frac{\nu^2(\nu_e^2 + \nu_0^2)}{(\nu_e^2 - \nu_0^2)^2}$$

$$F_B = \frac{2\nu^2(\nu_e\nu_s + \nu_0^2)}{(\nu_e^2 - \nu_0^2)(\nu_s^2 - \nu_0^2)}$$

The intensity of a particular band is proportional to the square of the appropriate frequency factor and in these equations $\nu_0$ is the laser frequency, $\nu_e$ and $\nu_s$ are the excitation frequencies to the two excited states, and $\nu = \nu_0 - \Delta\nu$, where $\Delta\nu$ is a vibrational quantum.

The $^2E_{1u} \leftarrow {}^2E_{2g}$ ferricenium electronic transition is electric dipole allowed and as such the $^2E_{1u}$ excited state could be the $|e^\circ\rangle$ state in a resonance Raman enhancement. Any vibrational modes that are strongly coupled to the $^2E_{1u} \leftarrow {}^2E_{2g}$ excitation would be enhanced in the Raman spectrum. For reasons given above, the symmetric ring–metal–ring tilt (368 cm$^{-1}$) should be coupled to the $^2E_{1u} \leftarrow {}^2E_{2g}$ excitation in the case of (DecaMFc$^+$)($PF_6^-$); however, the methyl carbon–hydrogen deformation (1422 cm$^{-1}$) would most likely *not* be strongly coupled to this electronic transition. Thus, for (DecaMFc$^+$)($PF_6^-$) the relative intensity of these two Raman lines should give an approximation as to the amount of enhancement in the tilt at 368 cm$^{-1}$. If the frequency dependence of this enhancement is studied, the energy separation ($E_{e^\circ} - E_{g^\circ}$) can be learned. Four laser lines were used for excitation, and in Figure 8 is plotted the relative intensity of the 368-cm$^{-1}$ band compared to the 1422-cm$^{-1}$ band. The $^2E_{1u} \leftarrow {}^2E_{2g}$ transition for (DecaMFc$^+$)($PF_6^-$) is at ~12,500 cm$^{-1}$ and since this is the only allowed transition at lower energy than 20,000 cm$^{-1}$, it is clear that it is involved in the scattering process. It is interesting that at 15,400 cm$^{-1}$, where the red line of the laser is used, no spectrum could be observed due to the high extinction coefficient of the sample at this frequency and the fact that pure undiluted solid samples were used. Dilute solution measurements may well allow a more complete study. The frequency dependence of the (DMFc$^+$)($TCA^-$)·2TCAA spectrum was also studied and a comparison of the intensities of the 322-cm$^{-1}$ symmetric ring–metal–ring stretch and the 432-cm$^{-1}$ $TCA^-$·2TCAA band gave similar results.

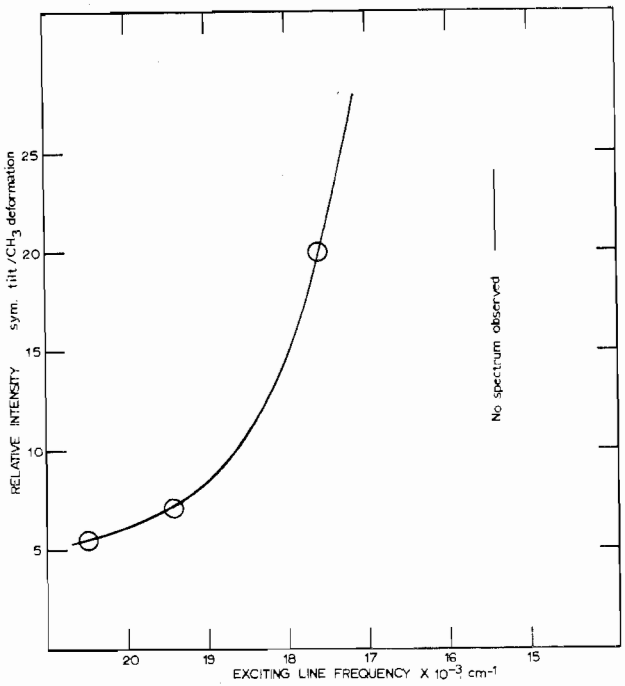


**Figure 8.** Resonance Raman enhancement for the symmetric ring–metal–ring tilt in (DecaMFc$^+$)($PF_6^-$) as gauged by a plotting of the relative intensity of the symmetric tilt compared to that of the $CH_3$ carbon–hydrogen deformation *vs.* the laser exciting frequency.

The frequency factors $F_A$ and $F_B$ can be used to predict the relative intensity of the various Raman lines as a function of the excitation frequency. If either $F_A$ or $F_B$ mimics the frequency dependency curve in Figure 8 better, then this would identify the resonance mechanism of primary importance. A calculation of the square of the frequency factor ($F_A^2$) for the three laser lines with which spectra were obtained for DecaMFc$^+$ with $\nu_e$ as the frequency of the $^2E_{1u} \leftarrow {}^2E_{2g}$ transition gives the relative values of 5.6 (blue line), 7.7 (green line), and 16.9 (yellow line). These relative numbers are probably within experimental error of the observed trend as set out in Figure 8, although it does seem that the observed intensity increase is somewhat greater than predicted by $F_A^2$.

In order to approximate $F_B^2$ the next lowest energy, dipole-allowed electronic state has to be identified as the $^2E_{1u} \leftarrow {}^2E_{2g}$ transition located[9] at 35,300 cm$^{-1}$. This second $^2E_{1u}$ excited state is taken as $|s^\circ\rangle$ and since both the lower energy $^2E_{1u}$ state, which is taken as $|e^\circ\rangle$, and $|s^\circ\rangle$ are of $^2E_{1u}$ symmetry, then they will be coupled by a totally symmetric vibrational mode. It is found that the resulting frequency dependence of the intensity is, in keeping with the findings of other workers, even less than that for the $F_A^2$ term. In fact, the $F_B^2$ intensities are essentially independent of frequency due to the location of the exciting line *between* the two electronic excited states. Therefore, the $F_A$ term best explains the

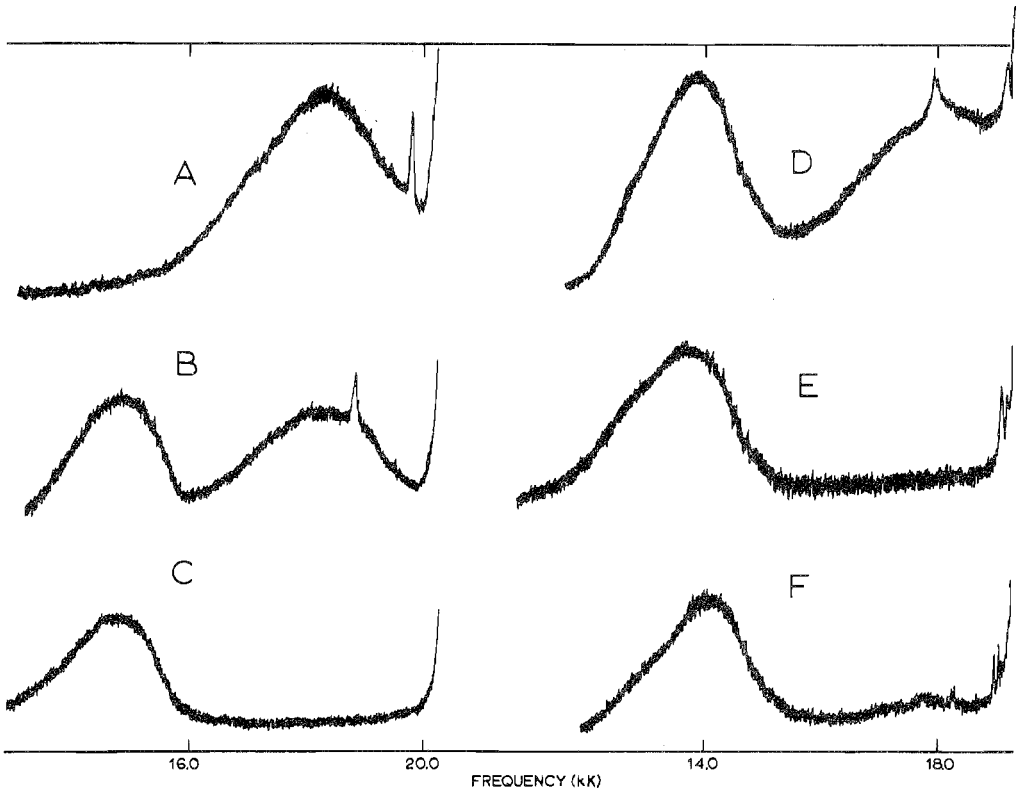


**Figure 9.** Wide-scan "Raman" spectra for rotating pressed pellets of $KPF_6$ (A), $(Fc^+)(PF_6^-)$ (B), $(Fc^+)(TCA^-)\cdot 2TCAA$ (C), $(DMFc^+)(PF_6^-)$ (D), $(DMFc^+)(TCA^-)\cdot TCAA$ (E), and $(TMFc^+)(PF_6^-)$ (F).

experimental curves and it is concluded that the resonance enhancement in $(DecaMFc^+)(PF_6^-)$ probably occurs due to excitation of the system into the lowest energy $^2E_{1u}$ state alone.

While carrying out Raman measurements on several of the ferricenium systems, it was noticed that very broad features could be seen, features that are believed to be molecular fluorescences. Figure 9 shows the wide-scan "Raman" spectra that were obtained for the various ferricenium compounds. The wide-scan spectrum for $KPF_6$ is also shown and it can be seen that there is a fluorescence at ~18,000 $cm^{-1}$ attributed to $PF_6^-$. Both of the $Fc^+$ systems show a broad feature at ~14,800 $cm^{-1}$; the feature moves to lower energies as the rings are alkylated: $(DMFc^+)(PF_6^-)$, 13,600 $cm^{-1}$; $(DMFc^+)(TCA^-)\cdot 2TCAA$, 13,780 $cm^{-1}$; $(TMFc^+)(TCA^-)\cdot 2TCAA$, 14,100 $cm^{-1}$. The fluorescence is from the lowest energy $^2E_{1u}$ state and in all cases the observed fluorescence occurs at lower energy than is found for the origin of the absorption (*vide infra*), which is to be expected if the ground-state geometry is different from that of the $^2E_{1u}$ excited state. It is intriguing that no fluorescence was observed for the $PF_6^-$ or $TCA^-\cdot 2TCAA$ salts of $DecaMFc^+$.

By way of summary and in anticipation of the next section, some relevant low-energy gerade frequencies for the various substituted ferrocenes and ferricenium systems are collected in Table VI (see Table V for the $DecaMFc^+$ systems). Bands that appear to be resonance Raman enhanced are indicated by an asterisk. It will be of considerable interest to see which vibrational modes are coupled to the $^2E_{1u} \leftarrow {}^2E_{2g}$ electronic transition as indicated by low-temperature electronic absorption spectroscopy.

**The $^2E_{1u} \leftarrow {}^2E_{2g}$ Transition.** The blue or green coloration of the various ferricenium ions is due in large part to the $^2E_{1u}[e_{1u}^3a_{1g}^2e_{2g}^4] \leftarrow {}^2E_{2g}[e_{1u}^4a_{1g}^2e_{2g}^3]$ electronic transition which appears in the region of ~12,000 to ~16,000 $cm^{-1}$ depending on the particular ferricenium ring substitution. The structure observed at low temperatures for this transition can be used[13-15] to gauge the low-symmetry (lower than $D_5$) distortional splitting of the $^2E_{1u}$ excited state into the two Kramers doublets $\psi_{\pm}{}^c$ and $\psi_{\pm}{}^d$ (separated in energy by the distortion parameter $\delta'$) and the energies of the $^2E_{1u}$ excited-state vibrations that are coupled to the $^2E_{1u} \leftarrow {}^2E_{2g}$ transition. As alluded to in the Introduction, this latter information can in turn be converted in a qualitative way to an understanding of the composition of the dominantly ring-based $e_{1u}$ orbital.[15] For example, the metal $4p_x$ and $4p_y$ orbitals are of $e_{1u}$ symmetry in the $D_{5d}$ point group. If there is little involvement of these two metal orbitals in the metal–ring bonding, then the metal–ring vibrational energies would be very similar for $^2E_{1u}$ ferricenium and $^1A_{1g}[e_{1u}^4a_{1g}^2e_{2g}^4]$ ferrocene. In fact, in our recent paper[15] just such an analysis was presented for the $^2E_{1u} \leftarrow {}^2E_{2g}$ vibrational structure seen for $(Fc^+)(PF_6^-)$, $(Fc^+)(TCA^-)\cdot 2TCAA$, and $(Fc^+)(BF_4^-)$ where from observed vibrational progressions the symmetric ring–metal–ring stretches ($\nu_4$) were found to be 303, 307, and 304 $cm^{-1}$, respectively (*cf.* the ferrocene value of 309 $cm^{-1}$). When observed, the symmetric ring–metal tilt $\nu_{16}$ also was found to be very close to the value found for ferrocene. On the contrary, the perpendicular ring bend ($\nu_{28}$) for the $^2E_{1u}$

**Table VI.** Summary of Relevant Symmetric Vibrational Frequencies ($cm^{-1}$) in Ferricenium Systems and Analogous Ferrocenes[a]

| Compd | $\nu_4$ | $\nu_{16}$ | $\nu_{28}$ |
|---|---|---|---|
| $FeCp_2$ | 308 | 391 | 599 |
| $(FeCp_2^+)(PF_6^-)$ | 304* | | |
| $(FeCp_2^+)(TCA^-)\cdot 2TCAA$ | 307* | | |
| DMFc | 318 | 330 | (402 and 631) |
| $(DMFc^+)(PF_6^-)$ | 311* | 327* | |
| $(DMFc^+)(TCA^-)\cdot TCAA$ | 322* | | |
| TMFc | 246* | 329 | |
| $(TMFc^+)(PF_6^-)$ | 218* | 316 | |
| $(TMFc^+)(TCA^-)\cdot 2TCAA$ | 218* | 311 | |

[a] The asterisk indicates resonance-enhanced bands; obviously, some bands are not strictly assignable to certain modes and the text should be consulted for individual assignments.

ferricenium state was found (~468 $cm^{-1}$ average) to be appreciably smaller than the 600-$cm^{-1}$ $^1A_{1g}$ ferrocene value in agreement with the ring-bonding character of the $e_{1u}$ orbital. It was also observed in these unsubstituted ferricenium ion studies that there were apparently more than the two expected electronic origins, *i.e.*, $\psi\pm^c(^2E_{1u}) \leftarrow \psi\pm^a(^2E_{2g})$ and $\psi\pm^d(^2E_{1u}) \leftarrow \psi\pm^a(^2E_{2g})$. In light of these observations on the electronic spectroscopy of $Fc^+$ and the above Raman and infrared work on the substituted ferricenium compounds, low-temperature electronic absorption measurements for the substituted ferricenium compounds were deemed potentially very useful.

For the substituted ferricenium species, shifts of the $^2E_{1u} \leftarrow {}^2E_{2g}$ origins to *lower* energy are seen in reference to the average origin positions found for $(Fc^+)(PF_6^-)$, $(Fc^+)(BF_4^-)$, and $(Fc^+)(TCA^-)\cdot 2TCAA$ at 15,715, 15,831, and 15,640 $cm^{-1}$, respectively. Since all of the substitutions are alkylations, the observed shift to lower energy is in qualitative agreement with the assigned ligand-to-metal charge-transfer character of the transition. In this section the low-temperature (some spectra were run at 4.2°K and they were found to be the same as those obtained at ~20°K) electronic absorption spectra for $(DMFc^+)(PF_6^-)$, $(DMFc^+)(TCA^-)\cdot TCAA$, $(TMFc^+)(TCA^-)\cdot 2TCAA$, $(TMFc^+)(PF_6^-)$, $(DecaMFc^+)(PF_6^-)$, and $(DecaMFc^+)(TCA^-)\cdot 2TCAA$ will be reported. Initially, the qualitative spectral characteristics will be presented with an eye to identifying the low-symmetry $^2E_{1u}$ distortion parameter $\delta'$. This will be followed by setting out the vibrational detail including Franck–Condon envelopes for some of the progressions.

For $(DMFc^+)(PF_6^-)$, the spectrum of which is illustrated in Figure 10, the principal vibrational progressions originate at peaks 1 (14,071 $cm^{-1}$) and 2 (14,234 $cm^{-1}$). Two weaker progressions can also be seen. The $(DMFc^+)(TCA^-)\cdot TCAA$ compound (lower tracing in Figure 10) seemingly has four clear origins at 14,384, 14,457, 14,526, and 14,556 $cm^{-1}$. It is interesting that all of the $^2E_{1u} \leftarrow {}^2E_{2g}$ transitions for the $TCA^-\cdot TCAA$ salt are at appreciably greater energies than those for the $PF_6^-$ salt. This probably is a reflection of the difference in ring configurations of the two $DMFc^+$ cations as we discussed in the previous sections. If the difference in transition energies is due to differences in ground-state energies, it could be said that the eclipsed rings in the $PF_6^-$ compound are tilted and the $e_{2g}(d_{x^2-y^2}, d_{xy})$ metal orbitals are now bonding more with the rings and the energy of the $e_{2g}$ molecular orbital is lowered. However, it is suspected that the magnitude of the difference is small enough to have many possible causes.

For $(TMFc^+)(PF_6^-)$, the best estimate of the origin position is 14,780 $cm^{-1}$, although the spectrum was only partially resolved, as shown in Figure 11. The spectrum of the $(TMFc^+)(TCA^-)\cdot 2TCAA$ salt, as illustrated in Figure 12, has four apparent origins (14,882, 14,970, 14,981, and 15,065 $cm^{-1}$) and they center at 14,972 $cm^{-1}$, which is ~200 $cm^{-1}$ different from the $PF_6^-$ compound. It seems that appreciable average origin energy differences can exist even when ground-state geometric differences are possibly quite small.

Both of the $DecaMFc^+$ salts start their first two vibrational progressions at 12,273 and 12,362 $cm^{-1}$, and the average origins of their four vibrational progressions are 12,385 $cm^{-1}$ for the $PF_6^-$ and 12,360 $cm^{-1}$ for the $TCA^-$ compound. The two spectra are reproduced in Figure 13. The similarity in these values for the two systems suggests that it might be possible to find clues to the identity of the four closely spaced excited states from which the four progressions arise.

In Table VII the apparent electronic origins found for the $^2E_{1u} \leftarrow {}^2E_{2g}$ transition for each of the nine compounds are reported. In Figures 10, 12, and 13 are indicated vibrational progressions that start from the various origins. Empirically we find that in the four cases where the vibrational features could be defined well enough to find four origins, that is for $(DMFc^+)(TCA^-)\cdot TCAA$, $(TMFc^+)(TCA^-)\cdot 2TCAA$, $(DecaMFc^+)(PF_6^-)$, and $(DecaMFc^+)(TCA^-)\cdot 2TCAA$, if the 1 and 4 positions and the 2 and 3 positions are averaged for each spectrum, it is found that in all cases the two averages are very close to identical. In other words the 1,4 and 2,3 pairs of transitions seem to be split from a common center of gravity. Another interesting observation is that in the $DecaMFc^+$ systems, while bands 1 and 2 have the same energy independent of the counterion, bands 3 and 4 change by 34 and 50 $cm^{-1}$, respectively, upon changing the counterion from $PF_6^-$ to $TCA^-\cdot 2TCAA$. A second observation can be made before speculation as to the details of the vibrational structure is advanced. As stated in the Introduction, it was thought that the energy levels in $DMFc^+$ and $TMFc^+$ should be similar due to the similar electronic properties of methyl and methylene moieties. This is the case for the $^2E_{1u} \leftarrow {}^2E_{2g}$ transitions of both $DMFc^+$ and $TMFc^+$ are shifted ~1000 $cm^{-1}$ from that for $Fc^+$. Additional methylation to give $DecaMFc^+$ leads to a ~2300-$cm^{-1}$ shift. It is concluded that a variety of different geometric distortions do not affect the $e_{2g}$ or $e_{1u}$ molecular orbitals anywhere near as much as do ring substitutions.

Table VII. Vibrational Origins for the $^2E_{1u} \leftarrow {}^2E_{2g}$ Transition in the Various Ferricenium Compounds[a]

| Compd | Origin position, $cm^{-1}$ 1 | 2 | 3 | 4 |
|---|---|---|---|---|
| $(Fc^+)(PF_6^-)$[b] | 15,596 | 15,833 | | |
| $(Fc^+)(BF_4^-)$[b] | 15,723 | 15,819 | 15,952 | |
| $(Fc^+)(TCA^-)\cdot 2TCAA$[b] | 15,552 | 15,731 | | |
| $(DMFc^+)(PF_6^-)$ | 14,071 | 14,234 | ? | ? |
| $(DMFc^+)(TCA^-)\cdot TCAA$ | 14,384 | 14,457 | 14,526 | 14,556 |
| $(TMFc^+)(PF_6^-)$ | 14,780 | | | |
| $(TMFc^+)(TCA^-)\cdot 2TCAA$ | 14,884 | (14,970)[c] | | 15,065 |
| $(DecaMFc^+)(PF_6^-)$ | 12,273 | 12,362 | 12,418 | 12,497 |
| $(DecaMFc^+)(TCA^-)\cdot 2TCAA$ | 12,273 | 12,362 | 12,384 | 12,447 |

[a] Origin positions are numbered in order; *i.e.*, the numbering does *not* indicate an assignment. [b] See ref 15. [c] Only an average position of no. 2 and 3 origins can be given due to overlapping and low intensities.

In part because of the appearance and centering of the 1,4 and 2,3 "origins" it is our present interpretation that the expected low-symmetry $^2E_{1u}$ excited-state splitting parameter $\delta'$ is to be gauged by the separation between the 1 and 4 origins. This leads to the conclusion that for all three $TCA^-$ salts studied the $^2E_{1u}$ excited-state splitting is 170–180 $cm^{-1}$, whereas for the $PF_6^-$ compounds $\delta'$ is in excess of 200 $cm^{-1}$ in each case. This is in accord with statements made earlier as to the relative packing merits of $TCA^-$ and $PF_6^-$. Previous work[15] gave $\delta'$ values of ~240 and 180 $cm^{-1}$ for $(Fc^+)(PF_6^-)$ and $(Fc^+)(TCA^-)\cdot 2TCAA$, respectively. It will be of interest to see if the low-symmetry $^2E_{2g}$ ground-state splitting parameter, as determined for instance by epr, will parallel the $^2E_{1u}$ $\delta'$ parameter. In this regard it is important to note that McCaffery and coworkers[16,17] have pointed out two important facts. First, the excited-state distortion $\delta'$ is resultant from an operator of different symmetry from that associated with $\delta$, the ground-state distortion parameter. Thus, if the ground state is distorted, the excited state need not be split proportionally or even in the same sense. The second relevant point is that the two excited-state Kramers doublets will give rise to absorption bands of different intensity, one weak and the other strong.

Additional information as to the identity of the excited states for the $^2E_{1u} \leftarrow {}^2E_{2g}$ transitions can potentially be obtained from the Franck–Condon contours of the various vibrational progressions. If the geometries of the excited and ground states are the same, then the (0, 0) vibrational component would be the most intense feature in a progression. A difference in

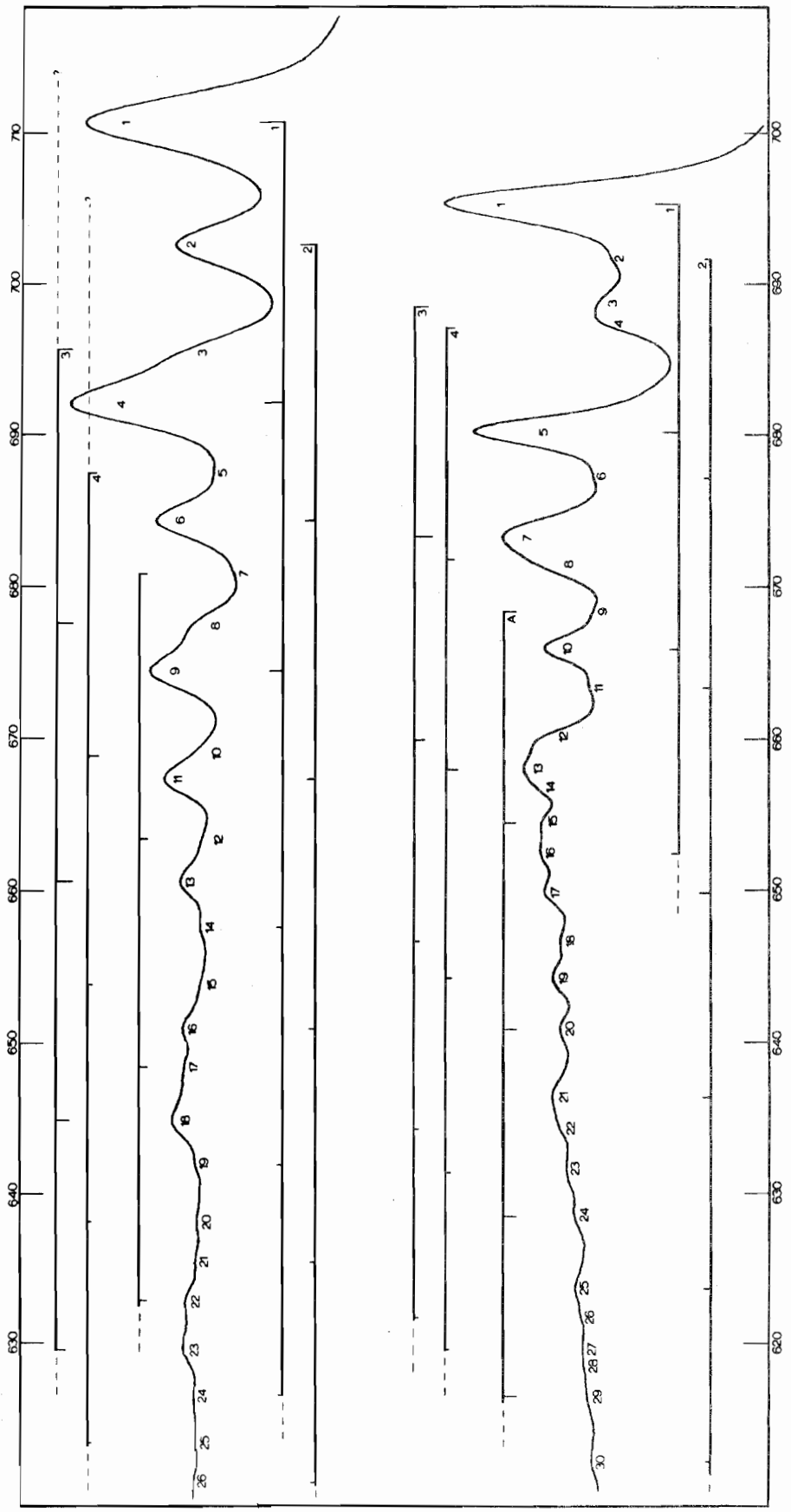


**Figure 10.** Low-temperature (~20°K) electronic absorption spectra of dilute KBr pellets of $(DMFc^+)(PF_6^-)$ (top) and $(DMFc^+)(TCA^-)\cdot TCAA$ (bottom). The numbers are used to identify peaks (see text) and for each spectrum five vibrational progressions are indicated.

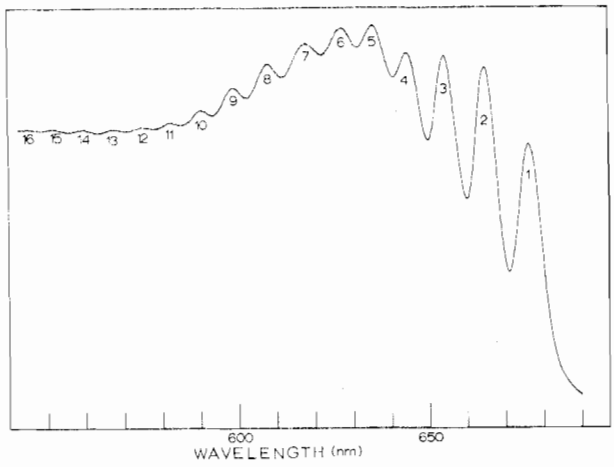


**Figure 11.** Low-temperature (~20°K) electronic absorption spectra of a dilute KBr pellet of $(TMFc^+)(PF_6^-)$.

geometries leads to the most intense component being other than the (0, 0). Plots of the Franck–Condon envelopes for the main progressions in $(DMFc^+)(PF_6^-)$, $(DMFc^+)(TCA^-)\cdot TCAA$, $(TMFc^+)(TCA^-)\cdot 2TCAA$, and $(DecaMFc^+)(PF_6^-)$ are shown in Figure 14. The plot for $(DecaMFc^+)(TCA^-)\cdot 2TCAA$ is not shown because it looks very similar to that for the other $DecaMFc^+$ compound. For the compounds $(DMFc^+)(PF_6^-)$ and $(TMFc^+)(TCA^-)\cdot 2TCAA$ progression number 1, which is always the strongest for all the ferricenium compounds, is characteristic of an excited state somewhat distorted from the ground state. For the other compounds the number 1 envelopes are characteristic of identical geometries. Inspection of all of the curves does not, unfortunately, suggest any pairwise (or otherwise) associations of progressions that work for all of the compounds. If the origins labeled 1 and 4 are properly assigned as the transitions to the split $^2E_{1u}$ state, then it is to be noticed that only in the $DecaMFc^+$ cases do both of the two excited states have geometries close to the ground state.

The presence of *four* electronic origins warrants an explanation because only the $\psi\pm^c(^2E_{1u}) \leftarrow \psi\pm^a(^2E_{2g})$ and $\psi\pm^d(^2E_{1u}) \leftarrow \psi\pm^a(^2E_{2g})$ transitions are expected since the $\psi\pm^b(^2E_{2g})$ Kramers doublet is *not* thermally populated. One possible explanation for four origins is that there are two different site symmetries in the unit cell for the ferricenium ions. There must be two crystallographically inequivalent types of cations *for each system*. Objections to this may be raised along the following lines. (1) It is unlikely that all five of the systems clearly showing four origins would have such similarly distributed states through such an "external" mechanism. (2) For several of the systems it would appear from the envelopes that if a two-site mechanism were accepted, one would have to justify the fact that one of the sites is more distorted than the other. (3) The crystallographic symmetry discussed for $(DMFc^+)(TCA^-)\cdot TCAA$ requires that all four molecules in the unit cell have the same environment; thus no site splitting is possible for this system.

Another possible explanation for the multiple origins is exciton splitting. The exciton coupling mechanism has been studied in many other systems.[42] A particular requirement for this splitting is that it takes place *via* interactions of molecules not related by merely translational operations in the lattice. For example, in the case of $(DMFc^+)(TCA^-)\cdot TCAA$ the four molelcules in the cell are not restricted to having parallel symmetry axes, and thus exciton splitting is not ruled out for this compound. A doping experiment might give a direct indication of the magnitude of this effect. $(Fc^+)(PF_6^-)$ was doped at the level of a few per cent into $(Co(cp)_2^+)(PF_6^-)$ and the visible spectrum was run at low temperatures. It was

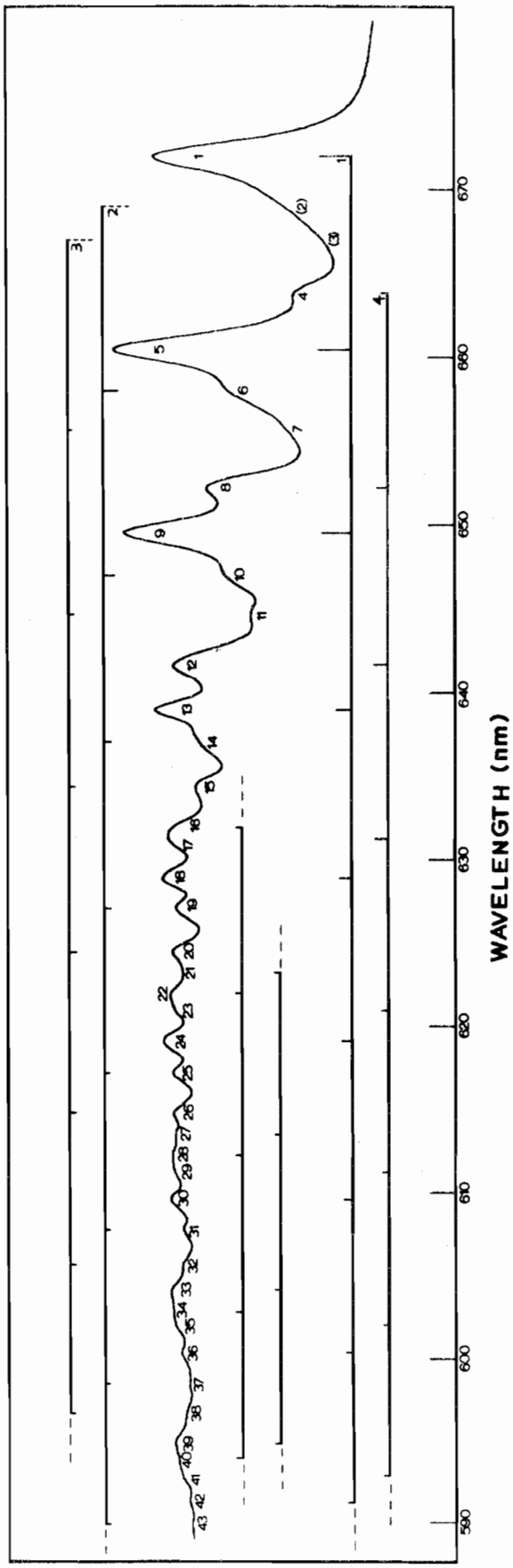


**Figure 12.** Low-temperature (~20°K) electronic absorption spectra of a dilute KBr pellet of $(TMFc^+)(TCA^-)\cdot 2TCAA$. Six vibrational progressions are indicated.

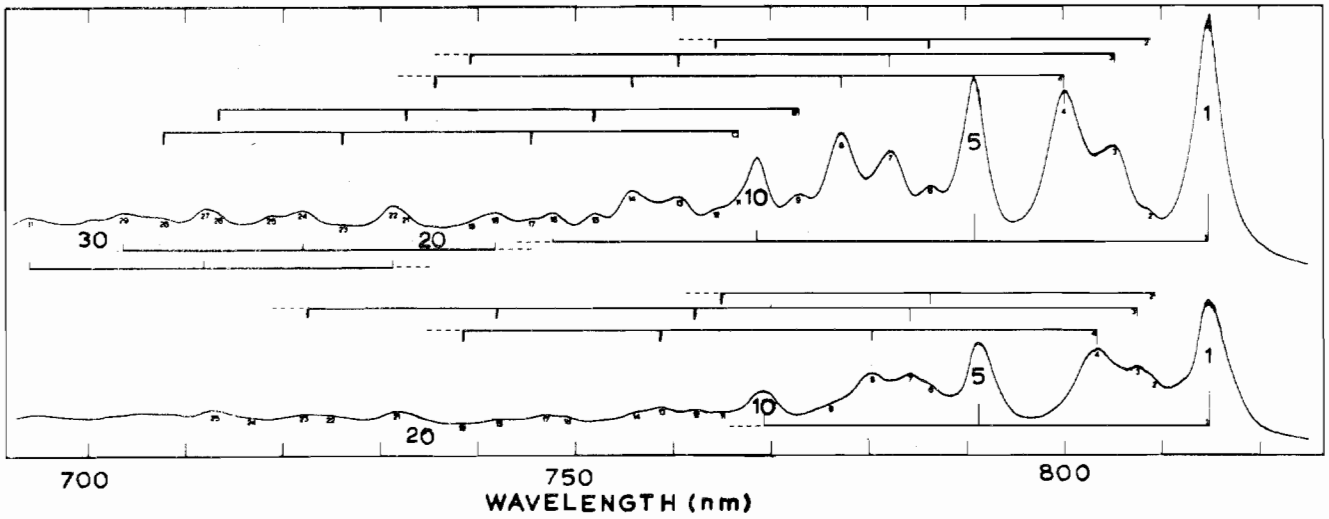


**Figure 13.** Low-temperature (~20° K) electronic absorption spectra of dilute KBr pellets of (DecaMFc$^+$)($PF_6^-$)(top) and (DecaMFc$^+$)-(TCA$^-$)·2TCAA (bottom). In each case four main vibrational progressions are indicated, and in the $PF_6^-$ case four additional progressions are identified.

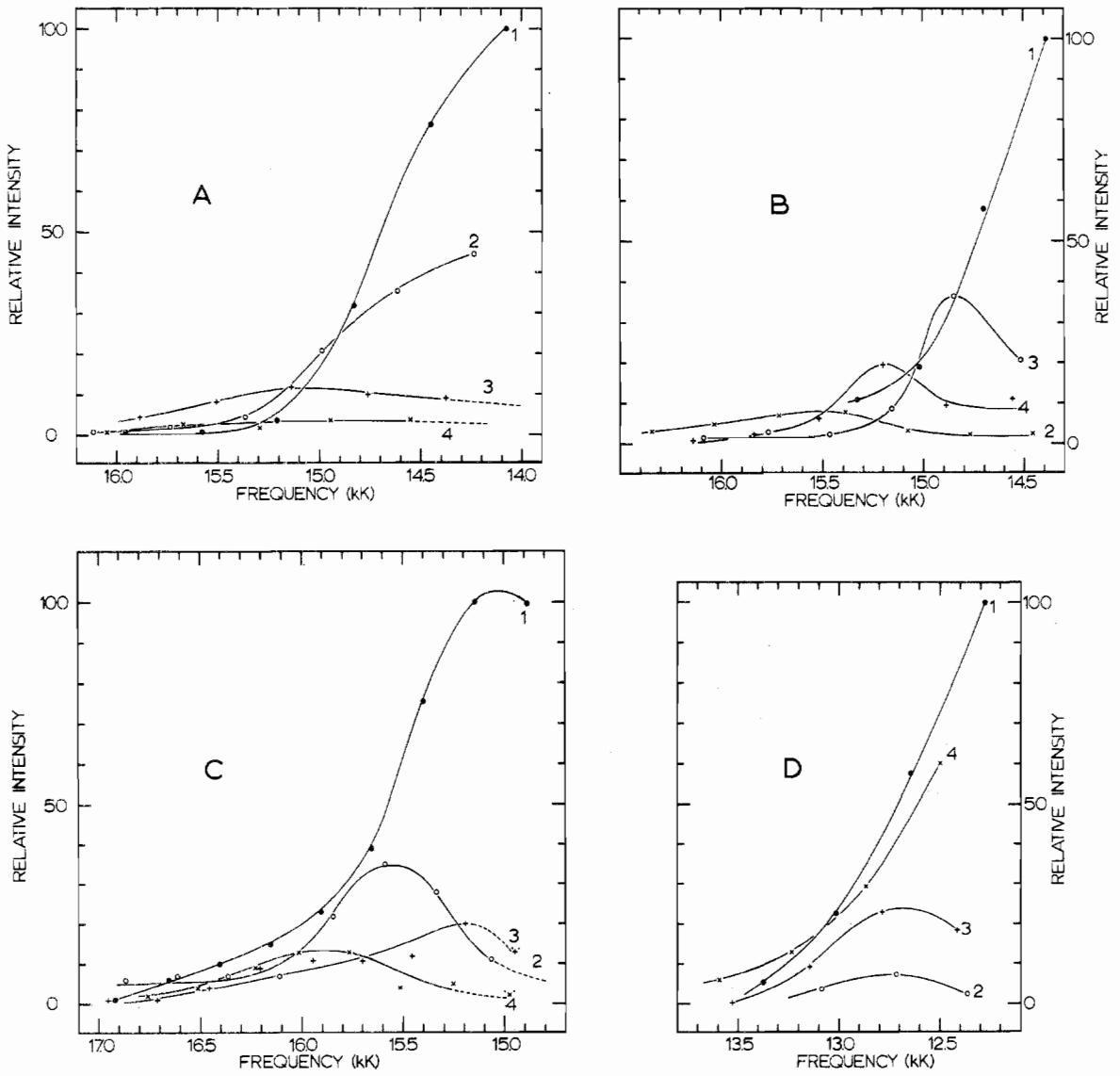


**Figure 14.** Franck-Condon envelopes for the four main vibrational progressions in the spectra of (DMFc$^+$)($PF_6^-$) (A), (DMFc$^+$)(TCA$^-$)·TCAA (B), (TMFc$^+$)(TCA$^-$)·2TCAA (C), and (DecaMFc$^+$)($PF_6^-$) (D).

found that, although considerably weaker than for the pure compound, the observed spectrum was equally well resolved and showed no differences in either intense or weak features. This is, of course, inconsistent with an exciton model where dipole–dipole interactions between ferricenium molecules would be expected to decrease as $r^{-3}$. Substituted cobalticenium salts were unavailable. The ideal experiment would be to study, including measurements of polarization, the doped single crystals of [Fe–Co(cp)$_2$](TCA)·2TCAA; however, due to the difficulty of obtaining [Co(cp)$_2$](TCA)·2TCAA crystals of suitable size and shape, this study could not be carried out.

A third possible explanation for some of the apparent electronic origins concerns the presence of low-energy librational modes. Hyams[33] very recently reported the observation of a relatively strong librational mode at 62 cm$^{-1}$ in the Raman spectrum of ferrocene. He also found three librational bands at 40, 52, and 60 cm$^{-1}$ for perdeuterated ferrocene. These same librational modes would be expected for the ferricenium ions; the potential well of the $\psi_{\pm}{}^{a}(^2E_{2g})$ Kramers doublet could be structured by various low-energy vibronic levels. If there is thermal population in, lets say, two different local minima of the $\psi_{\pm}{}^{a}(^2E_{2g})$ ground-state well, then there could be electronic transitions from both, and four electronic origins would be found. For example, the 1,4 origins could be resultant from one minimum in the $\psi_{\pm}{}^{a}$ well and the 2,3 origins from another. This does not seem to be the case, for we have *not* seen any appreciable intensity changes of certain low-energy peaks relative to others throughout the range where reasonable resolution is seen (easily 4.2–77°K). The $\psi_{\pm}{}^{c}(^2E_{1u})$ and $\psi_{\pm}{}^{d}(^2E_{1u})$ excited states could also be coupled to various low-energy librational modes and the two additional origins (*e.g.*, origins 2 and 3) are in fact two different (1, 0) vibrational components in two different librations and these two components have as their origin the intense, lowest energy origin 1. This would require that combination bands (libration plus some other vibration) would be visible from these two librational components, whereas no overtones of the librations would be seen. The corresponding librational components of the origin 4 would also be required to be nondetectable. All in all, the explanation employing librational modes seems quite inadequate and for now we can only say that further work is needed to understand the additional origins.

Independent of the assignment of the multiple electronic origins, it is possible and potentially very beneficial to investigate the vibrational progressions that are evident in Figures 10, 12, and 13. The electronic spectrum of (DMFc$^+$)(TCA$^-$)·TCAA is given in Figure 10 and the observed bands are given in Table VIII.[18] It is found that, for the two most easily measured of the four progressions, the initial spacings of the progressions labeled 1 and 3 are 317 and 322 cm$^{-1}$, which gives an average of 320 cm$^{-1}$. Because we have seen that the symmetric ring–metal–ring stretch in DMFc is 318 cm$^{-1}$ and also that it is 322 cm$^{-1}$ for the $^2E_{2g}$ ground state of (DMFc$^+$)(TCA$^-$)·TCAA, it is concluded that in this system *neither* the $e_{2g}$ *nor* the $e_{1u}$ orbital is appreciably bonding between the metal and the ring. This again is consistent with our earlier observation that the rings are probably close to parallel, as in ferrocene and unsubstituted ferricenium where similar conclusions about the $e_{2g}$ and $e_{1u}$ orbitals have been made.[15] A fifth ~320-cm$^{-1}$ progression labeled A in Table VIII[18] and Figure 10 is built on what may be one quantum of the perpendicular ring distortion frequency impressed on either the no. 1, 2, or 3 origin or possibly it is one quantum of symmetric ring tilt impressed on origin 4. Although there is no definite way to distinguish between these possibilities, the 578-cm$^{-1}$ perpendicular distortion frequency calculated if the no. 1 origin assignment is correct is probably too close to the DMFc value (631 cm$^{-1}$) to demonstrate adequately the ~130-cm$^{-1}$ reductions in this frequency that we have already seen[15] for the Fc$^+$ systems. And since a progression of this duration (*i.e.*, progression A) would not be expected to arise from origins with intensities as low as seen for 2 and 3, we would opt for assigning the A progression as the origin (4) + $\nu_{28}$ + $n\nu_4$, where $\nu_{28}$ (symmetric tilt) is 406 cm$^{-1}$. The closeness of this $\nu_{28}$ value to what is found in DMFc (402 cm$^{-1}$) correlates with both the assignment and previous discussion.

The case of (DMFc$^+$)(PF$_6^-$) is most unusual. As Table IX[18] and Figure 10 show, every detectable peak in this spectrum has been assigned as part of a progression stemming from one of four origins. The vibrational frequency of these progressions is found to be 379 cm$^{-1}$! This is indeed puzzling, for the Raman spectrum (Figure 3) of this compound indicated that both the symmetric ring–metal–ring stretch and the ring–CH$_3$ deformation are coupled to the $^2E_{1u} \leftarrow {}^2E_{2g}$ transition, and these lie at 311 and 327 cm$^{-1}$, respectively, in (DMFc$^+$)(PF$_6^-$) and 318 and 330 cm$^{-1}$, respectively, in DMFc. It is understandable that due to the tilting of the rings the $e_{1u}$ orbital would tend to bond with the metal, and by removing an $e_{1u}$ electron for the $^2E_{1u}$ excited state certain molecular frequencies would *decrease*, but at the moment it is not understood why it is that a change from the DMFc value by as much as 49–68 cm$^{-1}$ is observed and that the $^2E_{1u}$ vibrational energy is *greater*. As was found for the TCA$^-$ salt, there is a fifth ~379-cm$^{-1}$ progression which, although it cannot be identified due to the weakness of two of the origin peaks in this system, begins 619 cm$^{-1}$ from origin 1.

The electronic spectra of the 1,1'-trimethylene-bridged ferricenium systems have also presented some interesting results. The assignments of the bands in the (TMFc$^+$)(PF$_6^-$) and (TMFc$^+$)(TCA$^-$)·2TCAA systems are indicated in Tables X[18] and XI,[18] respectively. For the PF$_6^-$ salt the spectrum is poorly resolved and it can only be said that the initial peak spacing of 258 cm$^{-1}$ is probably within 10 cm$^{-1}$ of the energy of the individual progressions. However, it is to be noted that this corresponds to the 259-cm$^{-1}$ progressions found in the well-resolved TCA$^-$ spectrum. The listing below shows the frequencies of what has been assigned previously as a "torsion" mode for the three relevant states of TMFc and TMFc$^+$.

| $^1A_{1g}$, TMFc | $^2E_{2g}$, TMFc$^+$ | $^2E_{1u}$, TMFc$^+$ |
|---|---|---|
| 246 cm$^{-1}$ | 218 cm$^{-1}$ | 259 cm$^{-1}$ |

The explanation of the 218-cm$^{-1}$ band position entailed a suggestion that due to the bending of the rings the $e_{2g}$ orbital takes part in bonding to the ring. It was simplistically thought that the resonance enhancement of the 218-cm$^{-1}$ band in the Raman spectrum was possible through some component of metal–ring stretching being involved in the mode. The difference in frequencies between $^1A_{1g}$ TMFc and $^2E_{1u}$ TMFc$^+$ is somewhat reminiscent of what was found for (DMFc$^+$)(PF$_6^-$); the $^2E_{1u}$ frequency is higher, although in this case the difference of 13 cm$^{-1}$ is much smaller. In the TMFc systems it seems that even though the $e_{2g}$ orbital has become somewhat bonding in nature, the $e_{1u}$ orbital does not become appreciably involved in the metal–ring bonding. In other words, with respect to those molecular forces that determine the frequency of the so-called "torsion" mode, the increased overlap of the $e_{2g}$ orbital upon tilting the rings has a considerable strengthening effect, whereas the $e_{1u}$ overlap results in a decrease in the force constants.

In the case of the DecaMFc$^+$ systems vibrational progressions are seen at 370 and 367 cm$^{-1}$, respectively, for the PF$_6^-$ and TCA$^-$·2TCAA salts (see Tables XII[18] and XIII[18] and Figure 13). Recall that the Raman spectra of these two materials show symmetric tilts at 369 and 365 cm$^{-1}$, respectively, and the symmetric tilt for DecaMFc is 379 cm$^{-1}$. For these decamethylated molecules the difference between the $^1A_{1g}$ DecaMFc and $^2E_{2g}$ DecaMFc$^+$ frequencies was

explained above as being caused by bonding overlap of the $e_{2g}$ metal orbitals with the rings concurrent with the tilting motion. The $^2E_{1u}$ DecaMFc$^+$ frequencies are also reduced from the neutral molecule values and this suggests that the $e_{1u}$ orbital is involved in metal–ring bonding in much the same way as is the $e_{2g}$ orbital. Since all these differences are small, it should be stated that they are significant with respect to the error in measurements. The postulation of nearly equal $e_{2g}$ and $e_{1u}$ metal–ring bonding upon tilting of the rings seems to contrast with what was found for the TMFc$^+$ system. In that system for a *permanently* bent molecule the $e_{2g}$ orbital is more bonding than the $e_{1u}$ with respect to the forces involved in the *observed normal coordinate*. If it is a basically "torsion" mode that is involved in the TMFc$^+$ systems, it may be concluded that the $e_{2g}$ orbital in these systems is disposed such as to stabilize the rings to both tilting and twisting forces, while the $e_{1u}$ orbital does not change energy greatly as a function of twist or torsion.

Also in Tables XII[18] and XIII[18] are indicated for the DecaMFc$^+$ compounds two more progressions, B and C (see Figure 13). These are probably built on one quantum of perpendicular ring distortion from two of the origins.

**Epr Results.** Prins[6] has given $g$-value expressions appropriate for ferricenium systems

$$g_z = g_\parallel = 2 + 4k[-(\xi/\delta)/(1 + \xi^2/\delta^2)^{1/2}]$$

$$g_x = g_y = g_\perp = 2/(1 + \xi^2/\delta^2)^{1/2}$$

Here, $\xi$ is the spin–orbital coupling constant and $\delta$ is a one-electron splitting parameter gauging the effects of crystal fields lower in symmetry than $D_5$. The $g$ values for ferricenium systems are generally quite different from 2.0, a reflection of the presence of some orbital angular momentum, which is quenched as $\delta$ increases. Thus, for ferricenium derivatives with the largest low-symmetry distortions the $g$ values are closest to 2.0 and the effective magnetic moments approach the spin-only value of 1.73 BM. Epr can to be used to gauge the $\delta$ distortion parameter for the $^2E_{2g}$ ground state. It should be added here that for several years there was a running debate concerning the correct $g$ values for the ferricenium ion. While Wassermann[5,7] argued that impurities were giving rise to the signals reported by Prins, it is currently believed[8] that Prins' values are correct. This is supported in part by the epr data reported in this paper for (DecaMFc$^+$)(PF$_6^-$). The $g$-value arguments are reviewed by Anderson and Rai[8] and it is reported there that only Prins' values are consistent with their ferricenium and dimethylferricenium nmr contact shift data. It is quite possible that a dynamic pseudo-Jahn–Teller distortion could be present for a ferricenium ion;[43] however, it appears that our data do not warrant the consideration of such an effect.

The epr spectra obtained for pure powdered samples of the various substituted ferricenium systems at ~12°K are shown in Figure 15. There are two points to be made about the appearance of these spectra. First, for each of the spectra of the three trichloroacetate salts on the right side of Figure 15 there are weak features observed between the $g_\parallel$ and $g_\perp$ values. Although for the (DecaMFc$^+$)(TCA$^-$)·2TCAA case it is probable that some of the spectral features are due to the presence of impurities in the sample, it is clear that for the DMFc$^+$ and TMFc$^+$ trichloroacetates all unlabeled features are due to the fact that these samples are microcrystalline and could not be ground by hand sufficiently well to average completely over all crystallite orientations. The positions of all peaks intermediate between $g_\parallel$ and $g_\perp$ in the spectra of these two compounds were found to change upon rotation of the sample tube. Another observation of interest concerning the epr spectra relates to the line widths, particularly the comparison between the spectra of (TMFc$^+$)(PF$_6^-$) and (TMFc$^+$)(TCA$^-$)·2TCAA. No explanation will be advanced at this time for the variability in line width.

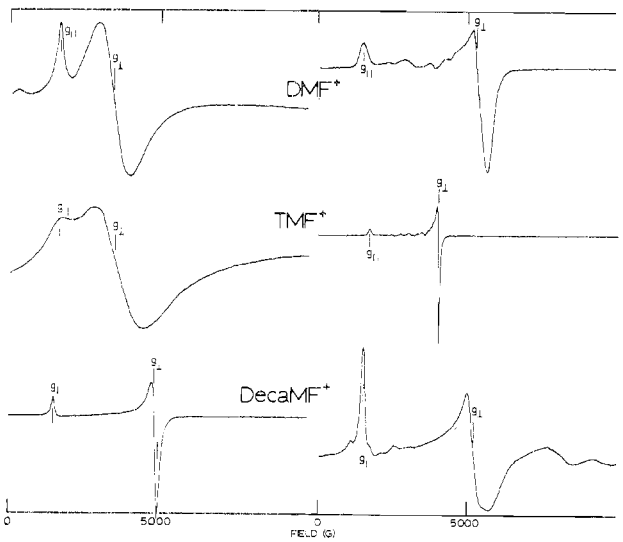


Figure 15. X-Band powder epr spectra for six substituted ferricenium compounds at ~12°K. The three spectra on the right are spectra for the three trichloroacetates, while the three on the left are those for the PF$_6^-$ salts.

Table XIV. Epr Data for the Various Ferricenium Systems

| Compd | $g_\parallel$ | $g_\perp$ | $\Delta_g$ | $\delta$, cm$^{-1}$ |
|---|---|---|---|---|
| (DMFc$^+$)(PF$_6^-$) | 4.002 | 1.92 | 2.08 | 1350 |
| (DMFc$^+$)(TCA$^-$)·TCAA | 4.44 | 1.22 | 3.22 | 310 |
| (TMFc$^+$)(PF$_6^-$) | 3.86 | 1.81 | 2.05 | 850 |
| (TMFc$^+$)(TCA$^-$)·2TCAA | 3.83 | 1.64 | 2.19 | 575 |
| (DecaMFc$^+$)(PF$_6^-$) | 4.433 | 1.350 | 3.083 | 365 |
| (DecaMFc$^+$)(TCA$^-$)·2TCAA | 4.37 | 1.26 | 3.11 | 324 |
| Fc$^+$ [a] | 4.35 | 1.26 | 3.09 | 322 |

[a] See ref 6.

Table XIV lists the $g$ values, $g$ anisotropy ($\Delta g$), and $\delta$ values for the various ferricenium ions. The distortion parameters reveal that in all cases the molecule is more distorted for the PF$_6^-$ counterion than with the TCA$^-$·$n$TCAA counterion. This is particularly true for the DMFc$^+$ systems, where the source of the difference in distortion has been mentioned in the Geometry section.

Evidence has been presented in the previous sections to show that the $^2E_{1u}$ excited-state low-symmetry parameter ($\delta'$) is also greater for PF$_6^-$ than TCA$^-$·$n$TCAA compounds. This relationship between $\delta$ and $\delta'$, although not a theoretically required one, is empirically borne out, and we can use the relationship to deduce the temperature dependence of $\delta$ from observation of electronic spectra at various temperatures. In our previous paper the spectra of (Fc$^+$)(PF$_6^-$) at 22, 83, and 119°K are shown. Although there is an appreciable loss in resolution as the temperature is raised, the positions of the first two most intense peaks (counterparts of origins 1 and 4) can reasonably be determined, and within experimental error they do *not* move relative to each other. We have assigned these peaks as transitions to the $\psi\pm^c$ and $\psi\pm^d$ Kramers doublets components of the $^2E_{1u}$ excited state, so the spacing between them is a gauge of $\delta'$. The temperature independence of these peaks then shows that the ground-state distortion parameter $\delta$ is most probably also independent of temperature. This is contrary to what has been claimed in the MCD ferricenium work,[16,17] where $\delta$ is reported to change by as much as a factor of 4 between 300 and 4°K; it is also contrary to the first suggestion of $\delta$ temperature dependence in the ferricenium magnetic susceptibility work.[4]

## Conclusion

Raman, infrared, low-temperature electronic absorption, and epr spectroscopies were used to study PF$_6^-$ and TCA$^-$ salts

**Table XV.** Summary of Spectroscopic Observables for Ferricenium Systems[a]

| Cation | Anion | Fe(II) Raman | Fe(III) Raman | $^2E_{1u}$ freq | $^2E_{1u}$ origins | Fluorescence band | $\delta'$ | $\delta$ |
|---|---|---|---|---|---|---|---|---|
| $FeCp_2^+$ | $PF_6^-$ | | 304 | 303 | 15,596, 15,833 | 14,800 | 233 | |
| $FeCp_2^+$ | $BF_4^-$ | 308, 391, 599 | | 304, 398, 471 | 15,723, 15,819, 15,952 | | 229 | 322 |
| $FeCp_2^+$ | $TCAA_3^-$ | | 307 | 307, 408, 466 | 15,552, 15,731 | 14,800 | 179 | |
| $DMFc^+$ | $PF_6^-$ | 318, 330 | 311, 327 | 379, ? | 14,071, 14,234, two more | 13,640 | >200 | 1350 |
| $DMFc^+$ | $TCAA_2^-$ | 402, 631 | 322 | 319, 406 | 14,384, 14,457, 14,526, 14,556 | 13,780 | 172 | 310 |
| $TMFc^+$ | $PF_6^-$ | 246, 329 | 218, 316 | ~258 | 14,780 | | | 850 |
| $TMFc^+$ | $TCAA_3^-$ | | 218, 311 | 259 | 14,884, 15,065, two at ~14,970 | 14,100 | 183 | 575 |
| $DecaMFc^+$ | $PF_6^-$ | 379, 590 | 369 | 370 | 12,273, 12,362, 12,418, 12,497 | | 224 | 365 |
| $DecaMFc^+$ | $TCAA_3^-$ | | 365 | 367 | 12,273, 12,362, 12,384, 12,447 | | 174 | 324 |

[a] All numbers are in $cm^{-1}$; $\delta'$ is the $^2E_{1u}$ state and $\delta$ the $^2E_{2g}$ state low-symmetry distortion parameter.

of a series of ferricenium cations. Important spectroscopic observables are summarized in Table XV. It should be recalled first of all that we are not able, through any of the techniques used, to study metal–ring bonding which involves the MO of $e_{1g}$ symmetry. This is unfortunate in that it is probably by far the most important bonding orbital in the system. However, we have studied the effective bonding of the $e_{2g}$ and $e_{1u}$ orbitals.

Vibrational spectroscopy of the neutral and oxidized molecule ground states has been shown to be consistent with little $e_{2g}$ metal–ring bonding in ferrocene and $Fc^+$ systems, and yet observable contributions from $e_{2g}$ bonding are deduced for the $(DMFc^+)(PF_6^-)$ and $TMFc^+$ cases. This is consistent with an increased $(d_{x^2-y^2}, d_{xy})$–ring overlap as the ring tilts.

Resonance Raman effects have shown which vibrational modes in each system are coupled to the $^2E_{1u} \leftarrow {}^2E_{2g}$ ring–metal charge-transfer transition. As Table XV indicates, different modes are probably coupled in the different systems.

The almost total assignment of vibrational structure on the $^2E_{1u} \leftarrow {}^2E_{2g}$ absorption band in the visible spectrum has allowed the measurement of vibrational frequencies of each molecular system in the $^2E_{1u}$ excited state. Comparing these frequencies to those found for the ground state, $^1A_{1g}$ neutral species led to the following conclusions. (1) In the $Fc^+$ systems no $e_{1u}$ or $e_{2g}$ orbital participation in metal–ring bonding is found. (2) The $(DMFc^+)(TCA^-)\cdot TCAA$ compound (with parallel rings) was found to have no $e_{2g}$ or $e_{1u}$ contributions. (3) The $DMFc^+)(PF_6^-)$ species gives evidence of only a small amount of $e_{2g}$ metal–ring bonding character but the metal $p_x$ and $p_y$ orbitals ($e_{1u}$ symmetry) interact with the ring $e_{1u}$ orbitals in such a way that the removal of $e_{1u}$ ring electrons *strengthens* the metal–ring bonding. (4) The $TMFc^+$ salts show evidence of substantial $e_{2g}$ bonding and an $e_{1u}$ "antibonding" effect similar to that found for the $(DMFc^+)(PF_6^-)$ material (the coupled vibrational mode in this case has been identified as more of a "torsion" motion than a ring–metal–ring stretch; therefore the *angular* bond strength properties of the $e_{2g}$ orbital are important in this case, in contrast to the systems above). (5) It was found that small, seemingly nearly equal $e_{2g}$ and $e_{1u}$ bonding contributions are made to the potential surface for tilting vibrations of the rings in $DecaMFc^+$ systems.

Several explanations were advanced for the multiple vibronic origins observed in the $^2E_{1u} \leftarrow {}^2E_{2g}$ band for all ferricenium-like molecules, but no explanation was found to be totally adequate. All in all it has to be said that regardless of whatever (partial) answers were provided for the questions stated in the Introduction an additional related question can be now added to the list.

The $^2E_{2g}$ ground-state distortion parameter ($\delta$) and that for the $^2E_{1u}$ excited state have been shown to be similarly dependent upon geometric perturbations of the system, even though they are not required to be so by symmetry considerations. From this information it was suggested that the temperature independence of the $(Fc^+)(PF_6^-)$ vibronic $^2E_{1u} \leftarrow {}^2E_{2g}$ spectrum implies insignificant temperature dependence of $\delta$.

**Acknowledgment.** We are grateful for partial funding of this research by National Institutes of Health Grant HL 13652. The Varian Model E-9 epr spectrometer and Spex Model RS2 Ramalab system were purchased, in part, by National Science Foundation departmental instrument grants.

**Registry No.** $(Fc^+)(PF_6^-)$, 11077-24-0; $(Fc^+)(TCA^-)\cdot 2TCAA$, 54182-35-3; $(DMFc^+)(PF_6^-)$, 51512-99-3; $(DMFc^+)(TCA^-)\cdot TCAA$, 54182-37-5; TMFc, 12302-04-4; $(TMFc^+)(PF_6^-)$, 54191-91-2; $(TMFc^+)(TCA^-)\cdot 2TCAA$, 54182-40-0; DecaMFc, 12126-50-0; $(DecaMFc^+)(TCA^-)\cdot 2TCAA$, 54182-43-3; $(DecaMFc^+)(PF_6^-)$, 54182-44-4; $Fe(cp)_2$, 102-54-5; DMFc, 1291-47-0; $(Fe(cp)_2^+)(BF_4^-)$, 1282-37-7.

**Supplementary Material Available.** Tables I, III, and VIII–XIII [analytical data, low-energy Raman data for ferricenium and cobalticenium compounds, and electronic spectra for $(DMFc^+)(TCA^-)\cdot TCAA$, $(DMFc^+)(PF_6^-)$, $(TMFc^+)(PF_6^-)$, $(TMFc^+)(TCA^-)\cdot 2TCAA$, $(DecaMFc^+)(PF_6^-)$, and $(DecaMFc^+)(TCA^-)\cdot 2TCAA$] and Figures 2, 4, and 6 [ir spectra of ferricenium complexes] will appear following these pages in the microfilm edition of this volume of the journal. Photocopies of the supplementary material from this paper only or microfiche (105 × 148 mm, 24× reduction, negatives) containing all of the supplementary material for the papers in this issue may be obtained from the Journals Department, American Chemical Society, 1155 16th St., N.W., Washington, D.C. 20036. Remit check or money order for $4.50 for photocopy or $2.50 for microfiche, referring to code number AIC40581F.

## References and Notes

(1) Esso Fellow, 1971–1972; Mobil Fellow, 1972–1973; University of Illinois Fellow, 1973–1974.
(2) Camille and Henry Dreyfus Fellow, 1972–1977.
(3) C. J. Ballhausen and H. B. Gray, "Coordination Chemistry," Vol. 1, American Chemical Society Monograph No. 168, American Chemical Society Publications, Washington, D.C., 1971.
(4) D. N. Hendrickson, Y. S. Sohn, and H. B. Gray, *Inorg. Chem.*, **10**, 1559 (1971).
(5) A. Horsfield and A. Wassermann, *J. Chem. Soc. A*, 3202 (1970).
(6) R. Prins and A. Kortbeek, *J. Organometal. Chem.*, **33**, C33 (1971).
(7) A. Horsfield and A. Wassermann, *J. Chem. Soc. A*, 187 (1972).
(8) S. E. Anderson and R. Rai, *Chem. Phys.*, **2**, 216 (1973).
(9) Y. S. Sohn, D. N. Hendrickson, and H. B. Gray, *J. Amer. Chem. Soc.*, **93**, 3603 (1971).
(10) D. N. Hendrickson, *Inorg. Chem.*, **11**, 1161 (1972).
(11) D. W. Turner in "Physical Methods in Advanced Inorganic Chemistry," H. A. O. Hill and P. Day, Ed., Interscience, New York, N.Y., 1968.
(12) J. W. Rabalais, L. O. Werme, T. Bergmark, L. Karlsson, M. Hussain, and K. Siegbahn, *J. Chem. Phys.*, **57**, 1185 (1972).
(13) Y. S. Sohn, D. N. Hendrickson, and H. B. Gray, *J. Amer. Chem. Soc.*, **92**, 3233 (1970).
(14) R. Prins, *Chem. Commun.*, 280 (1970).
(15) D. N. Hendrickson, Y. S. Sohn, D. M. Duggan, and H. B. Gray, *J. Chem. Phys.*, **58**, 4666 (1973).
(16) M. D. Rowe, R. Gale, and A. J. McCaffery, *Chem. Phys. Lett.*, **21**, 360 (1973).
(17) M. D. Rowe and A. J. McCaffery, *J. Chem. Phys.*, **59**, 3786 (1973).
(18) Supplementary material.
(19) J. W. Bats, J. J. deBoer, and D. Bright, *Inorg. Chim. Acta*, **5**, 605 (1971).
(20) T. Bernstein and F. H. Herbstein, *Acta Crystallogr., Sect. B*, **24**, 1640 (1968).
(21) R. C. Petterson, Ph.D. Thesis, University of California, Berkeley, Calif., 1966.
(22) E. A. Siebold and L. E. Sutton, *J. Chem. Phys.*, **23**, 1967 (1955); J. D. Dunitz, L. E. Orgel, and A. Rich, *Acta Crystallogr.*, **9**, 373 (1956).

(23) A. Schlueter, D. M. Duggan, D. N. Hendrickson, and H. B. Gray, unpublished results.
(24) "International Tables for X-Ray Crystallography," Vol. I, Kynoch Press, England, Birmingham, 1952–1962.
(25) N. D. Jones, R. E. Marsh, and J. H. Richards, *Acta Crystallogr.*, **19**, 330 (1965).
(26) H. P. Fritz, *Advan. Organometal. Chem.*, **1**, 267 (1964).
(27) E. R. Lippincott and R. D. Nelson, *Spectrochim. Acta*, **10**, 307 (1958).
(28) T. V. Long, Jr., and F. R. Huege, *Chem. Commun.*, 1239 (1968).
(29) D. Hartley and M. J. Ware, *J. Chem. Soc. A*, 138 (1969).
(30) J. Bodenheimer, E. Loewenthal, and W. Low, *Chem. Phys. Lett.*, **3**, 715 (1969).
(31) J. Brunvoll, S. J. Cyvin, and L. Schäfer, *J. Organometal. Chem.*, **27**, 107 (1971).
(32) I. J. Hyams, *Spectrochim. Acta, Part A*, **29**, 839 (1973).
(33) I. J. Hyams, *Chem. Phys. Lett.*, **18**, 399 (1973).
(34) I. Pavlik and J. Klickorka, *Collect. Czech. Chem. Commun.*, **30**, 664 (1965).
(35) P. Sohar and J. Kuszmann, *J. Mol. Struct.*, **3**, 359 (1969).
(36) R. T. Bailey and E. R. Lippincott, *Spectrochim. Acta*, **21**, 389 (1965).
(37) G. Herzberg, "Infrared and Raman Spectra," Van Nostrand, New York, N.Y., 1945.
(38) A. C. Albrecht, *J. Chem. Phys.*, **34**, 1476 (1961).
(39) J. Tang and A. C. Albrecht, *Raman Spectrosc.*, **2**, Chapter 2 (1970).
(40) A. C. Albrecht and M. C. Hutley, *J. Chem. Phys.*, **55**, 4438 (1971).
(41) W. Kiefer and H. J. Bernstein, *Mol. Phys.*, **23**, 835 (1972).
(42) D. S. McClure, "Electronic Spectra of Molecules and Ions in Crystals," Academic Press, New York, N.Y., 1959.
(43) J. H. Ammeter and J. D. Swalen, *J. Chem. Phys.*, **57**, 678 (1972); J. H. Ammeter and J. M. Brom, Jr., *Chem. Phys. Lett.*, **27**, 380 (1974).

Contribution from the Chemical Physics Group, Tata Institute of Fundamental Research, Bombay 400005, India

# Paramagnetic Anisotropy and Electronic Structure of $S = {}^3/_2$ Halobis(diethyldithiocarbamato)iron(III). I. Spin-Hamiltonian Formalism and Ground-State Zero-Field Splittings of Ferric Ion

P. GANGULI, V. R. MARATHE, and S. MITRA*

*Received September 11, 1974* AIC40641H

The paper describes the results of paramagnetic anisotropy measurements on the single crystals of a series of halobis(diethyldithiocarbamato)iron(III) in which the ferric ion is in the intermediate spin state. A convenient method is given to calculate the "rhombic" principal molecular anisotropies from the measured crystalline quantities of a monoclinic system and is applied to calculate the molecular anisotropies of these molecules. An important result of the present measurements is the discovery of a large "in-plane" anisotropy in these molecules. Using spin-Hamiltonian formalism, the $g_i$ values and zero-field splitting (ZFS) parameters ($D$ and $E$) of the ground state of the ferric ion ($^4$A) have been determined. The ($E/D$) ratios are observed to be large and decrease from the chloro to the iodo derivative. The total ZFS (in cm$^{-1}$) is deduced to be 3.36, 16, and 19.1 for the chloro, bromo, and iodo derivatives, respectively.

## I. Introduction

An intermediate spin state for a $3d^5$ ion ($S = {}^3/_2$) is rather a rare occurrence, the low ($S = {}^1/_2$) and high ($S = {}^5/_2$) spin states being the most common ones. It may be primarily because of this reason that the magnetic properties and electronic structure of $S = {}^3/_2$ halobis(dialkydithiocarbamato)iron(III) have been of great interest. Single-crystal X-ray structural studies are now available on different halogenodiethyl derivatives.[1-4] The molecular geometry is essentially the same in all cases and is diagramatically shown in Figure 1. The iron atom in these molecules has a highly distorted square-pyramidal geometry, the halogen being at the apex of the pyramid and the iron atom at the center, about 0.6 Å above the mean rectangular basal plane of the four sulfur atoms belonging to the dithiocarbamate (dtc) ligands. The dtc ligands are not coplanar with each other, but they are so with the iron atom. The local symmetry at the iron site is low and is close to $C_2$.

Extensive low-temperature average magnetic susceptibility,[4-6] Mössbauer,[4,5,7-9] and some esr[4,10] studies have been reported on several derivatives of the above series. The average magnetic susceptibility of all of these molecules in the liquid nitrogen temperature range obeys the Curie law very closely and conforms to the spin state of $S = {}^3/_2$ for the ferric ion. The presence of any significant exchange interaction is evident only below 4°K or so. The results of the Mössbauer and esr studies have been interpreted to establish that the ground electronic state of the ferric ion in this system is a spin quartet orbital singlet. In addition, the single-crystal esr study on the isopropyl homolog has given an estimate of the zero-field splitting (ZFS) of the ground state. A very accurate and direct estimate of the ZFS in some of these molecules is available from far-infrared spectroscopy studies.[11,12] These measurements are generally done in the liquid helium temperature range and hence are often handicapped because of the presence of magnetic-exchange interactions.

A detailed crystal field calculation is now available, in which an attempt has been made to rationalize the available experimental results on these molecules on the basis of $C_{4v}$ symmetry.[13] In these calculations, a scheme for the ordering of energy levels for the ferric ion has been proposed. As will become apparent later, there are some serious discrepancies in these calculations.

The present work was undertaken to deduce the ground- and excited-state electronic properties of the ferric ion from the measurements of paramagnetic anisotropy between 80 and 300°K on the chloro, bromo, and iodo derivatives of the diethyl homolog, abbreviated here as $Fe(dtc)_2X$ (X = Cl, Br, I). In this paper detailed experimental results of the paramagnetic anisotropy measurements on the $Fe(dtc)_2X$ series are presented, a method of calculating molecular anisotropy is outlined, and finally the values of ZFS and other parameters are calculated using spin-Hamiltonian formalism. A preliminary report of the paramagnetic anisotropy study on $Fe(dtc)_2Cl$ has been published.[14]

## II. Experimental Section

The compounds were prepared by the reported method.[1,6] Large well-developed single crystals ($\sim 10 \times 4 \times 2$ mm$^3$) were obtained by slow evaporation of a 80:20 chloroform–toluene solution. It has been observed that this ratio was rather critical in getting good-quality, large single crystals. The crystals grow as elongated prisms with the long axis as the $c$ axis. The crystals, particularly the iodo derivative,